HHS Public Access

Author manuscript

Brain Struct Funct. Author manuscript; available in PMC 2016 May 01.

Published in final edited form as:

Brain Struct Funct. 2015 May ; 220(3): 1511–1528. doi:10.1007/s00429-014-0741-9.

A novel form of ciliopathy underlies hyperphagia and obesity in *Ankrd26* knockout mice

Peter Acs,
Laboratory of Molecular Biology, National Cancer Institute, NIH, Bethesda, USA

Peter O. Bauer,
Neuro-oncology Branch, National Cancer Institute, National Institute of Neurological Disorders and Stroke, National Institutes of Health, Bethesda, USA

Balazs Mayer,
Adult Stem Cell Unit, CSDB, National Institute of Dental and Craniofacial Research, NIH, Bethesda, USA

Tapan Bera,
Laboratory of Molecular Biology, National Cancer Institute, NIH, Bethesda, USA

Rhonda Macallister,
National Cancer Institute, NIH, Bethesda, USA

Eva Mezey, and
Adult Stem Cell Unit, CSDB, National Institute of Dental and Craniofacial Research, NIH, Bethesda, USA

Ira Pastan
Laboratory of Molecular Biology, National Cancer Institute, NIH, Bethesda, USA

Eva Mezey: mezeye@mail.nih.gov

Abstract

Human ciliopathies are genetic disorders caused by mutations in genes responsible for the formation and function of primary cilia. Some are associated with hyperphagia and obesity (e.g., Bardet–Biedl Syndrome, Alström Syndrome), but the mechanisms underlying these problems are not fully understood. The human gene *ANKRD26* is located on 10p12, a locus that is associated with some forms of hereditary obesity. Previously, we reported that disruption of this gene causes hyperphagia, obesity and gigantism in mice. In the present study, we looked for the mechanisms that induce hyperphagia in the *Ankrd26*−/− mice and found defects in primary cilia in regions of the central nervous system that control appetite and energy homeostasis.

Correspondence to: Eva Mezey, mezeye@mail.nih.govacspeti@yahoo.com.

E. Mezey and I. Pastan contributed equally to the work.

Electronic supplementary material The online version of this article (doi:10.1007/s00429-014-0741-9) contains supplementary material, which is available to authorized users.

Keywords

Obesity; Neuronal cilia; Leptin receptor; ANKRD26; Melanocortin receptor; Feeding behavior; Paraventricular nucleus; Arcuate nucleus; CRH; Ciliary body proteins

Introduction

Almost all mammalian cells have a primary cilium, a cellular antenna that senses a wide variety of signals (Singla and Reiter 2006). Ciliary defects have been shown to underlie a variety of disorders with distinct clinical features (e.g., retinal degeneration; polydactyly; situs inversus; mental retardation; encephalocele; polycystic kidney, liver, and pancreas). Some ciliopathies are also associated with hyperphagia and obesity; e.g., Bardet–Biedl syndrome (BBS) (Benzinou et al. 2006) and Alström syndrome (Collin et al. 2002). The connection between primary cilia and obesity was initially established in 2003 when genes responsible for BBS were identified and their protein products were found in the basal body (Ansley et al. 2003; Grace et al. 2003), a protein complex at the base of the primary cilium (Seo et al. 2011). The basal body plays crucial role in transporting proteins including G-protein-coupled receptors and adenylyl cyclase 3 (AC3), the most specific ciliary marker, from the cytoplasm to the primary cilia.

The *ANKRD26* gene is located on chromosome 10p12 in humans, a locus associated with certain forms of genetic obesity (Dong et al. 2005). In a previous study, we described the phenotype of mice with defects in the *Ankrd26* gene. These mice display hyperphagia, severe obesity, gigantism, and elevated serum leptin levels (Bera et al. 2008). Leptin, which is released following meals by white adipose tissue, inhibits appetite by activating “anorexogenic” nerve cells in the hypothalamic arcuate nucleus (ARC) (Fig. 1). These cells release appetite-suppressing peptides (α-MSH, which is derived from the POMC precursor, and CART). Leptin also inhibits the activity of a separate population of “orexigenic” cells in the ARC that release NPY and AGRP. Both the anorexigenic and orexigenic cells send axonal projections to small (parvocellular) neurons in the hypothalamic paraventricular nucleus (PVN) as well as other nuclei in the medial and lateral hypothalamus.

Alpha-MSH (a peptide cleaved from POMC in the ARC upon leptin activation) is the natural agonist of melanocortin 4 receptors (MC4R) and is one of the most potent anorexigenic peptides. Alpha-MSH analogs are capable to rescue the extreme obese phenotype of POMC knockout mice. Alpha-MSH mainly acts on cells with MC4 receptors in the PVN and induces marked appetite reduction by promoting the production of several peptides that suppress appetite: corticotropin-releasing hormone (CRH), thyrotropin-releasing hormone (TRH), and oxytocin. Contrary to alpha-MSH, AGRP inhibits the MC4R and the consequent reduction in appetite; thus, a decrease in its secretion results in an increase in the activity of the MC4R-positive cells in the PVN (Beckers et al. 2009; Raciti et al. 2011; Valassi et al. 2008). The remarkable role of the above-mentioned peptides and receptors in the regulation of food intake is clearly demonstrated by knockout obesity models. Mutations in the genes that encode leptin (Friedman and Halaas 1998), the leptin receptor (Chua et al. 1996), POMC (Yaswen et al. 1999), or the MC4R (Huszar et al. 1997)

all lead to hyperphagia and obesity in both humans (Beckers et al. 2009, 2010) and rodents. So do lesions that destroy both PVNs (Leibowitz et al. 1981).

Based on these findings, we wondered whether *Ankrd26*−/− mice might have defects in the ARC and/or PVN that could account for their phenotype. For this purpose, we tested the distribution of Ankrd26 in the brain and its presence in the anorexigenic cell populations in the hypothalamus. Additionally, we tested the functionality of the leptin–POMC–alpha-MSH pathway and the stress pathway in *Ankrd*26−/−mice.

Results

Distribution of Ankrd26 in the central nervous system

To begin to understand the phenotype of the *Ankrd26*−/− mouse, we first analyzed the expression of Ankrd26 in the brain by in situ hybridization and immunohistochemistry (IHC). We found that both the Ankrd26 protein and its mRNA are widely distributed in the mouse CNS (Fig. 2). Because the knockout mice suffer from obesity and gigantism, we focused on areas known to be involved in feeding behavior. In the hypothalamus, the PVN and the ARC had the strongest Ankrd26 staining. Strong signals were also detected in the dorsomedial (DM) and ventro-medial (VM) nuclei. In the brainstem, the nucleus of the solitary tract (NTS)—a recognized feeding center (Grill and Hayes 2009)—exhibited the most robust staining along with the dorsal raphe nucleus. Ankrd26 was also present in the cortex, in the hippocampal dentate gyrus, CA1 region (weakly), and in the CA2 and CA3 regions (high levels). Limbic structures such as the amygdala, mammillary bodies, and the habenula had fairly intense staining as well. Outside the CNS, Ankrd26 was also co-expressed in the pituitary ACTH cells (Fig. 3).

In summary, Ankrd26 is expressed in neuronal cell bodies and their processes, and in glial cells in feeding centers of the hypothalamus as well as areas of the brain that project to these centers (e.g., NTS).

Leptin targets in the ARC of *Ankrd26*−/− mice

Even though adult *Ankrd26*−/− mice have elevated serum leptin levels, they remain hyperphagic. In other words, they fail to respond to a signal that should suppress their appetite. This could be the result of a marked decrease in the production and release of α-MSH.

Dual immunohistochemical labeling demonstrated that leptin receptor-expressing cells and POMC-producing cells in the ARC as well as the MC4R-expressing cells in the PVN co-expressed Ankrd26 (Fig. 3). To confirm the specificity of leptin receptor and MC4R antibodies, we performed combined IHC and in situ hybridization and found significant overlap between the labelings (Supplementary Fig. 1).

We used a micro punch technique (Palkovits 1973) to study the expression of neuropeptides in isolated hypothalamic nuclei. Microdissected ARC, PVN, and cortical samples were used for quantitative (q) RT-PCR analysis. While we found no changes in the ARC in the expression of POMC between the WT and *Ankrd26*−/− mice, both AgRP and NPY mRNA

levels were significantly reduced in the *Ankr26*−/− mice (Supplementary Table 1). Since NPY Y1 (Y1R) and Y2 (Y2R) receptors have been suggested to have a role in the regulation of food intake (Mercer et al. 2011), we also measured their expression. Y1R (but not Y2R) mRNA levels were significantly reduced in the PVN of the *Ankrd26*−/− mice (Supplementary Table 1).

These data suggest a compensatory decrease or impaired activation of the expression of these neuropeptides.

Even though we found no differences in POMC mRNA levels in the WT vs. knockout mouse ARC, we still wondered whether hyperphagia might be induced by reduced levels of α-MSH there because α-MSH levels can be altered without an obvious change in POMC expression (Lloyd et al. 2006). α-MSH is the natural agonist of MC4Rs and it has a strong anorexigenic effect (Tung et al. 2006). Upon leptin activation α-MSH is cleaved from POMC in the ARC neurons (for details see Fig. 4a) (Wardlaw 2011). To test the leptin responsiveness of the ARC POMC neurons, we measured α-MSH levels in the hypothalamus in 6-week-old mice. As compared to WT mice, the *Ankrd26*−/− mice had significantly higher body weights and elevated leptin levels (Fig. 5a, b). As reported in our previous study, no other metabolic changes were observed in these mice (Raciti et al. 2011). In line with the elevated leptin levels, significantly higher α-MSH in the hypothalami of the *Ankrd26*−/− mice was detected (Fig. 5c).

The data mentioned above suggest intact leptin responsiveness at the age of 6 weeks in the *Ankrd26*−/− mice. The phosphorylation of STAT3 (signal transducer and activator of transcription 3) following leptin activation has been well documented and accepted as a sign of intact leptin responsiveness in the ARC after leptin administration (Bates et al. 2003). To confirm that the physiological response to leptin is maintained at the age of 6 weeks in *Ankrd26*−/− mice, we injected mice either with leptin or saline intraperitoneally and analyzed STAT3 phosphorylation in the ARC using IHC. In the ARC of the leptin-treated mice, we found an intense, nuclear P-STAT3 staining in both *Ankrd26*−/− and WT mice with no difference between the two groups (Fig. 5d). In the saline-treated mice, only a few cells exhibited P-STAT3 staining and it was quite weak.

These findings indicate that the leptin responsiveness in *Ankrd26*−/− mice remains intact and that the melanocortin pathway must be affected further downstream, most likely in the PVN, of these mice.

All the results above suggest that no changes in the arcuate nucleus could explain hyperphagia. Thus, we continued to explore other possibilities.

Changes in the MC4 receptor for α-MSH in the PVN

Since cells in the ARC appear to be leptin responsive and since their responses to leptin did not seem to be grossly abnormal, we wondered whether the functional defect in the *Ankrd26*−/− mice was in the PVN instead of the ARC. To answer this question, we initially looked at MC4Rs in PVN cells. MC4R mRNA was decreased in microdissected PVN nuclei in *Ankr26*−/−mice vs. WT (Supplementary Table 1).

Obese, hyperphagic *Pomc*−/− mice (with functional MC4Rs are preserved) lose weight when they are treated with α-MSH (Yaswen et al. 1999). Since the *Ankrd26*−/− mice exhibit hyperphagia even though they have high leptin and α-MSH levels, we wondered whether an Ankrd26 deficiency affects the function of MC4R. To test this hypothesis, we recorded the body weight (BW) of *Ankrd26*−/−, *Pomc*−/− and WT mice in a 2-week pretreatment period and then treated them with either α-MSH or vehicle (PBS). The *Ankrd26*−/−, *Pomc*−/−, and WT mice gained comparable amounts of weight during the control period. However, during the 2-week treatment period, both the α-MSH- and the PBS-treated *Ankrd26*−/− mice continued to gain weight, while the α-MSH-treated *POMC*−/− mice lost weight (Fig. 5e). α-MSH administration significantly slowed the weight gain of WT mice; PBS-treated WT mice showed similar weight gains during the pretreatment and treatment periods.

These results show that the MC4R is indeed dysfunctional in *Ankrd26*−/− mice and suggested that the deletion of Ankrd26 affects the function of the melanocortin pathway.

Characterization of primary ciliary markers in *Ankrd26−/−* mice

The melanocortin pathway is known to be altered in primary ciliopathies characterized by primary hyperphagia and obesity (Rahmouni et al. 2008; Wang et al. 2009). The decrease in MC4R levels in the PVN hinted that neurons there might suffer from a ciliopathy. To test this hypothesis, we visualized primary ciliary markers, including AC3, Mchr1 and Sstr3, in wild-type and *Ankrd26*−/− mice. Almost all PVN neurons in the WT brains contained AC3-positive primary cilia (Fig. 6a); in the PVN of the *Ankrd26*−/− mice no ciliary AC3 staining was observed in the parvocellular region, and in the magnocellular areas there were only occasional very short “stumps” observed (Fig. 6b). In addition to the lack of staining in the PVN, a significant reduction of AC3 staining was seen in the suprachiasmatic, DM and VM nuclei of the *Ankrd26*−/− mice, while no obvious difference was observed in other areas including the ARC nucleus (Fig. 6c, d). AC3-positive primary cilia numbers were significantly decreased in the amygdala and hippocampus as well as in the cerebral cortex in the *Ankrd26*−/− mice (Supplementary Table 2).

Next, we investigated the expression of the two appetite-related ciliary receptors: Mchr1 and Sstr3. Mchr1 immunostaining was markedly lower in the PVN of the knockout mice (Fig. 6e, f), but not in the accumbens nucleus, where Mchr1 is highly expressed (Berbari et al. 2008a). Almost all cells in the hippocampal CA1 and CA2 regions and in the amygdala exhibit Mchr1 on their primary cilia in WT mice, but this receptor could not be detected in the CA1 and CA2 regions of *Ankrd26*−/− mice (Supplementary Table 2).

Although the Sstr3 could only be detected on a few primary cilia in the PVN of WT mice, immunostained cilia in the PVN seemed to be even rarer in *Ankrd26*−/− mice. Sstr3 staining was also significantly reduced in the VM nucleus (Fig. 6g–l) while there was no difference in the DM and ARC nuclei. In the limbic system, we observed a slightly decreased immunostaining in the central amygdala and in all areas of the cortex of *Ankrd26*−/− mice, while there was no change in Sstr3 expression in the hippocampus and the rest of the amygdala (Supplementary Table 2).

These data suggest a region-specific reduction in the expression of primary cilium-specific proteins in *Ankrd26*−/− mice.

Expression and subcellular localization of specific structural ciliary proteins in the brains of WT and *Ankrd26*−/− mice

Alterations in the expression of ciliary markers (AC3 and cilia-specific GPCRs) suggested that the transport of ciliary proteins might be impaired in the *Ankrd26*−/−mice. We studied the presence and distribution of proteins specific to the BBSome—a protein complex, which is a part of the basal body of primary cilia—especially proteins Bbs2 and Bbs4, which play a crucial role in transporting GPCRs (e.g., Mchr1 and Sstr3) to the cilia (Blacque and Leroux 2006; Berbari et al. 2008b). We also examined rootletin, a protein involved in ciliary transport mechanisms, and assembling and maintaining ciliary rootlets (Yang et al. 2002).

Bbs2 showed a punctate staining in the brains with no obvious differences between the WT and the *Ankrd26*−/− mice. We observed a similar punctate staining of Bbs4 in the brains of WT mice, a pattern that is typically seen in physiological conditions (Kim et al. 2004). In *Ankr26*−/− mice, however, we found unusually strong cytoplasmic Bbs4 staining in the brain areas (PVN, DM, VM, cortex, CA3) where the expression of AC3, Mchr1, and Sstr3 were reduced (Fig. 7).

Immunostaining of rootletin also revealed significant differences between the WT and the *Ankr26*−/− mice. In the hypothalamic PVN, VM and ARC as well as in limbic system areas (hippocampal CA3 region and amygdala) diffuse, weak staining was observed in WT mice. Cytoplasmic staining was markedly increased in the *Ankrd26*−/− mice. Additionally, structures that looked like ciliary rootlets were detected in the KO, but not in WT mice (Supplementary Fig. 2). This might result from a compensatory upregulation of rootletin and/or impaired targeting of this protein to the rootlets.

These data suggest that the intracellular distributions and physiological functions of Bbs4 and rootletin might be abnormal in the absence of Ankrd26.

Role of Ankrd26 in the melanocortin pathway

Since it has been reported that ciliary defects in BBS affect the function of the melanocortin pathway leading to leptin-resistant obesity (Rahmouni et al. 2008; Wang et al. 2009; Guo and Rahmouni 2011) we wondered which appetite-related neuronal pathways are affected by the ciliopathy and MC4R dysfunction in *Ankrd26*−/− mice. To answer this question, we studied the expression of appetite-related neuropeptide mRNAs in hypothalamic nuclei of *Ankrd26*−/− mice. The qRT-PCR results indicated clear differences in the expression of neuropeptides between the WT and *Ankrd26*−/− mice (Supplementary Table 1). To identify areas potentially involved in these changes, we performed in situ hybridization in serial sections because this provides high-resolution, cellular information about the distribution of neuropeptide mRNAs. The experiments were performed in two age groups. In the 4-week-old (not yet obese) *Ankrd26*−/− mice, we investigated primary alterations leading to excessive food consumption, since these mice exhibit hyperphagia at this age, but have the same body weight (BW) and leptin levels as age- and gender-matched WT mice. The other

group consisted of 3-month-old mice with the typical phenotype of *Ankrd26*−/− mice (obesity, elevated leptin levels, etc.). The older animals were used to search for mechanisms that might be responsible for maintaining hyperphagia.

No differences were found between *Ankrd26*−/− and WT mice in POMC mRNA in the ARC in either age group. In agreement with our qRT-PCR result, NPY expression in the ARC was reduced in mutant mice in both age groups (Fig. 8a, b). Interestingly, neurons in the hypothalamic DM nucleus of 3-month-old mutant mice expressed NPY, while it was absent in the WT mice (Fig. 8i–k).

AgRP expression was slightly reduced in *Ankrd26*−/− mice in both age groups in the ARC (Fig. 8c, d).

To look for malfunctions in the appetite-related pathways regulated by MC4Rs in the PVN (Fig. 4) (Lu et al. 2003; Harris et al. 2001; Sabatier et al. 2003), we measured CRH, TRH and oxytocin mRNAs in the PVN. In agreement with our qRT-PCR study, CRH was strongly upregulated in the mutant mice (Fig. 8e, f) while TRH and oxytocin expression was unchanged in both age groups (data not shown). At 3 months of age, TRH mRNA was strongly increased in the brainstem midline raphe nuclei (Fig. 8l–n). It has been described, that NPY-producing hypothalamic DM neurons project to brain stem TRH neurons and induce hyperphagia by activating the dorsal motor vagus complex (Ao et al. 2006; Yang et al. 2009). Our data suggest that the activation of this pathway contributes to the over eating in *Ankrd26*−/− mice.

The increased expression of CRH in the PVN (Fig. 8e, f) suggests that the HPA axis is likely to be involved in producing the hyperphagia and obesity in the *Ankrd26*−/− mice. Since arginine vasopressin (VP) is also found in CRH-producing cells in the parvocellular PVN, and it also participates in regulating the HPA axis (Itoi et al. 2004; Kiss et al. 1984; Sawchenko et al. 1984), we decided to look for changes in VP mRNA. In situ hybridization revealed that in the WT PVN, VP was expressed predominantly in magnocellular cells, with only a few VP-labeled parvocellular cells. On the other hand, in the Ankrd26−/− mice, the expression of VP was elevated in both magno- and parvocellular cells in the PVN in both young and older mice (Fig. 8g, h).

Studying the stress pathway

a. Serum ACTH and corticosterone levels—Alterations in neuropeptides in the hypothalamic parvocellular PVN suggested that regulation of the HPA axis is affected by the *Ankrd26* deletion, so we decided to test the function of the stress pathway. First, we measured the basal serum levels of ACTH and corticosterone (CORT) and found that both are significantly elevated in the *Ankrd26*−/− mice (Fig. 9a, b upper panels) in unstressed animals. After 15 min of restraint stress, ACTH and CORT increased in the serum of WT and knockout mice, but the levels achieved were significantly higher in the *Ankrd26*−/− mice (Fig. 9a, b lower panels) suggesting that their HPA axis is overly sensitive.

b. Effect of adrenalectomy on body weight—We have shown that the medial parvocellular subdivision of the PVN, where the CRH neurons are located, lacks AC3 in

their primary cilia in the *Ankrd26*−/− mice (Fig. 6). In addition, these mice have significantly higher brain CRH and serum CORT levels. Therefore, we asked whether an altered HPA axis might contribute to the hyperphagia seen in these animals. We performed adrenalectomies (ADX) in WT and *Ankrd26*−/− mice, and used sham-operated animals as controls. Half of the ADX mice and half of the controls received CORT supplementation. To confirm the successful adrenalectomy and the effectiveness of CORT supplementation, we measured the CORT concentration in the serum of adrenalectomized and CORT-supplemented mice. The average CORT concentration was 5.08 ± 2.1 ng/mL in ADX *Ankrd26*−/− mice and 5.3 ± 1.9 ng/mL in ADX WT mice. In CORT-supplemented animals, it was 80.6 ± 16 ng/mL and 70.7 ± 15 ng/mL in knockout and WT mice, respectively. The BW of unsupplemented (ADX), CORT-supplemented (ADX + CORT) and sham-operated (SHAM) mice was monitored for 54 days. The changes in the body weights of the animals in the various treatment groups from the 14th day until the end of the experiment are shown in Fig. 9c.

In the first 14 days following the adrenalectomies all of the *Ankrd26*−/− mice lost weight. After their initial weight loss, the *Ankrd26*−/− mice started to gain weight again and at the end of the experiment, all reached their original body weights. There was no significant difference in the body weight among the members of *Ankrd26*−/− groups at any time point. The WT mice also lost weight in the first postoperative 14 days. The body weights of WT ADX mice were 90 ± 2 % of their initial values by the end of the experiment. In contrast, the WT ADX + CORT and the WT SHAM groups regained their original BW. At the end of the experiment, the BW of the WT ADX group was significantly lower than their initial weight ($p = 0.006$) and than the weight of the WT ADX + CORT ($p = 0.007$) and the WT SHAM ($p = 0.03$) groups.

These data suggest that the regulation of appetite is independent of peripheral CORT levels in *Ankrd26*−/− mice.

Discussion

Obesity and related comorbidities are global medical challenge (Friedman 2000). Environmental factors contribute to the increased obesity worldwide. However, numerous gene mutations can cause syndromes that include obesity (e.g., MC4R, LepR, BBS, Alström Syndrome, Prader Willi Syndrome, Cohen syndrome, Carpenter syndrome, Fragile X Syndrome) (Goldstone and Beales 2008), but such mutations are uncommon. There is a growing body of evidence suggesting that genetic factors have a more influential role in determining the body weight than considered before (Wardle et al. 2008). Consequently, there is an urgent need to find candidate genes that might directly regulate the energy homeostasis and influence the susceptibility to obesity (Ramachandrappa and Farooqi 2011). Identification of such genes could open new avenues for therapeutic management of obese patients.

The most prominent phenotypic features in the *Ankrd26*−/− mice are hyperphagia, obesity and gigantism (Bera et al. 2008). In the present study, we investigated the underlying mechanisms leading to this phenotype. We found that deletion of the C-terminus of the

protein encoded by *Ankrd26* leads to severe region-specific changes in primary cilia in the brain, resulting in the disruption of the function of the melanocortin pathway and the HPA axis and leading to excessive food intake and obesity.

Ciliopathy

Mutations resulting in ciliopathies are associated with obesity (Benzinou et al. 2006), but the relationship between the genetic alteration and the phenotype is poorly characterized. Based on the obese phenotype of the *Ankrd26*−/− mice we wondered whether Ankrd26 could be involved in primary ciliary function. We found profound regional changes in the distribution of primary ciliary markers (AC3, Mchr1 and Sstr3) between WT and *Ankrd26*−/− mice. The most profound change in the *Ankrd26*−/− mice was the absence of AC3-positive primary cilia in the PVN (Fig. 6), one of the most important feeding centers in the brain (Fig. 4). The role of AC3, a specific constituent of and marker for primary cilia in the CNS, in the regulation of appetite has been established in both humans and in mice. Genetic variations at the AC3 locus in humans are associated with obesity and type2 diabetes (Nordman et al. 2008). In mice, deletion of the *Ac3* gene induces hyperphagia and obesity (Wang et al. 2009). Besides AC3, the dysfunction of basal body proteins is involved in human ciliopathies accompanied by obesity. The human ciliopathy, BBS is characterized by mutations in the BBS genes that affect the physiological function of the basal body, and dysfunctional basal body is implicated in the development of the hyperphagia and obesity in these patients (Benzinou et al. 2006; Ansley et al. 2003). Additionally, Guo et al. suggest that ciliar pathology induces impaired melanocortin pathway (namely impaired leptin receptor function) in human ciliopathy BBS (Guo and Rahmouni 2011). In accordance with these findings, we assume that dysfunctional primary cilia promote the disruption of the melanocortin pathway in *Ankrd26*−/− mice, although not at the level of leptin receptor, but at MC4Rs.

We feel that the impaired expression of ciliary proteins AC3, Mchr1 and Sstr3 in feeding centers of *Ankrd26*−/− mice might be a result from disrupted basal body function. *Ankrd26*−/− mice mimic the *Bbs2*−/− and *Bbs4*−/− mice in their phenotype and lack of ciliary markers Mchr1 and Sstr3 on their primary cilia (Berbari et al. 2008b). Failure of basal body protein, Bbs4 to function properly could account for decreases in the numbers of ciliary receptors Mchr1 and Sstr3 in the *Ankrd26*−/− mice (Fig. 6). Mchr1 and Sstr3 are GPCRs with well-characterized roles in the regulation of energy balance and body weight (Saito et al. 2001). In fact, ablation of *Bbs2* or *Bbs4* leads to the loss of ciliary localization of these GPCRs and the absence of Mchr1 and Sstr3 from the primary cilia induces hyperphagia and obesity in *Bbs2*−/− and *Bbs4*−/− mice (Berbari et al. 2008b). It seems that Ankrd26 is required, perhaps as a scaffold protein, for the ability of Bbs4 to recognize and transport target proteins. In the absence of Ankrd26, Bbs proteins do not appear to be incorporated into the cilia, and they build up in the cytoplasm of affected cells with disrupted primary cilia (Fig. 7). Additionally, the region-specific overexpression and altered distribution of rootletin—a prominent ciliary protein with a role in ciliary transport mechanisms (Yang and Li 2005)—further suggest that the lack of functional Ankrd26 disrupts the basal bodies and inhibits ciliary transport. Based on these observations, we

suggest that Ankrd26 has a general role in maintaining the protein complex that is responsible for ciliary assembly.

Ciliopathy and hyperphagia: the role of the PVN

Next, we asked which feeding-related neuronal pathways might be affected by the pathological ciliary function and are responsible for the hyperphagia in *Ankrd26*−/− mice. The presence of Ankrd26 in cells that comprise the melanocortin pathway and the remarkable reduction of ciliary proteins in the PVN suggested that the lack of functional Ankrd26 and the consequent ciliopathy impairs the most important anorexigenic pathway, the melanocortin pathway and particularly the MC4R-expressing PVN neurons.

The physiological regulation of the melanocortin pathway is illustrated in Fig. 4. Briefly, when leptin activates pro-opiomelanocortin (POMC)-producing neurons in the ARC, α-MSH synthesis and release are stimulated. Alpha-MSH acts on MC4 receptors in the PVN and exerts its anorexigenic effects by activating CRH, TRH and oxytocin neurons and thus inhibits appetite (de Backer et al. 2011; Pandit et al. 2011). As demonstrated in Fig. 5, in *Ankrd26*−/− mice elevated leptin levels are accompanied by physiological phosphorylation of STAT3 and elevated hypothalamic α-MSH levels indicating that the leptin response and the melanocortin pathway is intact. Despite elevated α-MSH levels, *Ankrd26*−/− mice exert hyperphagia and MC4R mRNA levels are decreased in their PVN and in the pituitary gland. The administration of the strong MC4R agonist α-MSH did not prevent the excessive food intake. Based on the above data, we assume that the ciliopathy in the *Ankrd26*−/− mice might in fact disrupt the function of the MC4Rs in the PVN. Under physiological conditions, increased expression of MC4R in the PVN indicates the activation of melanocortin anorexigenic system, which would prevent the mice from overfeeding (Stofkova et al. 2009). Thus, the reduced expression of MC4R in *Ankrd26*−/− mice may suggest an impaired activation of the melanocortin system at the level of the PVN and cannot protect the animals from overfeeding. These findings suggest that the MC4R function in the PVN is disrupted in *Ankrd26*−/− mice and this impaired melanocortin pathway contributes to the hyperphagia.

Besides its role in the regulation of food intake, the PVN—in particular the CRH and VP neurons—plays a crucial role in the control of the HPA axis as well. The CRH and VP cell groups in the PVN are activated by stress stimuli and inhibited by CORT, which terminates the stress response on multiple levels (pituitary gland, ARC, PVN) (Itoi et al. 2004; Kiss et al. 1984; Sawchenko et al. 1984). We propose that impaired expression of primary ciliary markers in the PVN is associated with the inability of CRH neurons to sense peripheral CORT levels leading to overactivation of CRH neurons, disrupted MC4R function, and inducing hyperphagia in the *Ankrd26*−/− mice. Proper MC4R function requires physiological CNS steroid response (Sebag and Hinkle 2006); thus, the MC4R dysfunction may be induced by impaired CORT sensing mechanism in the PVN of *Ankrd26*−/− mice.

Our data indicate that the CNS CORT sensing mechanism is indeed impaired in the *Ankrd26*−/− mice, as elevated CRH and VP levels in the PVN are accompanied by increased peripheral ACTH and CORT levels and the stress response of *Ankrd26*−/− is enhanced compared to the WT mice. These findings indicate that the downstream CRH pathway (ACTH secretion by the pituitary gland and consequent CORT production by the adrenals)

is over-activated in *Ankrd26*−/− mice and suggest an impaired negative feedback by CORT inducing CRH and VP overproduction. Interestingly, the neuropeptide profile of the *Ankrd26*−/− mice (low ARC NPY and AgRP, high PVN CRH and VP) is characteristic for the post-adrenalectomy state, where the peripheral levels of CORT are negligible (Savontaus et al. 2002).

Based on these findings, we propose that the PVN of *Ankrd26*−/− mice is resistant to corticosterone; regulation of energy metabolism in the animals reflects an adaptation to the absence of the central effects of CORT. To confirm that the regulation of energy homeostasis is independent of central CORT effects, we performed ADX, and found that the absence of CORT indeed did not affect the body weight of the *Ankrd26*−/− mice and that the body weight changes of the ADX (CORT-depleted state) and CORT-replaced KO mice were identical.

The impaired CNS CORT sensing mechanism in *Ankrd26*−/− mice induces hyperphagia at multiple levels. As recently reported, overexpressed CRH in the PVN can induce hyperphagia in itself (Nakayama et al. 2011). Additionally, it has been demonstrated that intact CNS CORT is required for proper MC4R function (Sebag and Hinkle 2006) and dysfunctional MC4Rs in the *Ankrd26*−/− mice clearly contribute to the hyperphagia.

Interestingly, the CRH cell population in the PVN is a mutual crossing point of the anorexigenic melanocortin pathway and the stress axis (Fig. 4) (Lu et al. 2003). As shown in Fig. 10, MC4R-expressing CRH neurons in the PVN are highly ciliated in WT mice, but AC3-positive primary cilia are absent in these cells in *Ankrd26*−/− mice. Based on these findings, our data suggest that one of the key cell populations responsible for the phenotype in *Ankrd26*−/− mice is the CRH-producing, MC4R-expressing cell group in the PVN.

The role of ARC NPY cells

In addition to the overexpression of CRH and VP in the PVN, the impaired CNS CORT sensing mechanism in the *Ankrd26*−/− mice also results in reduced ARC NPY levels, since under physiological conditions CORT activates the ARC NPY neurons (Palkovits 2008) and NPY exerts an inhibitory effect on the CRH cells in the PVN and contributes to the termination of the stress response (Dimitrov et al. 2007). The low ARC NPY levels activate a well established orexigenic pathway (Yang et al. 2009; Ao et al. 2006) in *Ankrd26*−/− mice: DM neurons start to produce NPY (Fig. 8), and NPY—acting on brain stem TRH neurons (Fig. 8)—induces hyperphagia through the dorsal motor nucleus of the vagus nerve. This pathway is also known to be activated in *Mc4r*−/−, obese mice (Arens et al. 2003) supporting the suggestion that impaired MC4R function could be important in the *Ankrd26*−/− mice.

Conclusions

Recent work has suggested that neuronal ciliary dysfunction contributes to human obesity in Bardet–Biedl syndrome (BBS) but the underlying molecular and cellular mechanisms remained obscure. Several BBS proteins are responsible for intracellular protein/vesicle trafficking including targeting several receptors to the cilia (Seo et al. 2009). Mutations in

genes that directly influence the expression of signaling (e.g., AC3) or structural proteins (e.g., proteins of the basal body) of the primary cilia induce disturbances in energy homeostasis in both humans and mice (Sen Gupta et al. 2009). However, Ankrd26 is the first example of a *non-cilium-specific* protein that is required to prevent the development of a ciliopathy associated with morbid obesity. We feel that Ankrd26 might be a part of the transport system for ciliary proteins, working specifically as a member of a gating or scaffolding complex. When it is mutated or deleted, cilia-targeted proteins such as AC3, Mchr1 or Sstr3 cannot be incorporated into the primary cilia and thus cannot fulfill their physiological functions. The result is impaired appetite regulation and stress management.

Our findings suggest that membrane and/or scaffold proteins are required for the proper primary ciliary function and by their (currently mostly unknown) mutations ciliopathies might represent a broader spectrum of genetic obesity than previously considered. Our data provide a novel mechanism for genetic obesity and might supply new targets, diagnostic and therapeutic approaches to human obesity syndromes.

Experimental procedures

Mice

Ankrd26−/− mice were produced as described previously (Bera et al. 2008). C57BL/6 wild-type mice were purchased from the Jackson Laboratory (USA). Mice were kept at standard conditions, typically three or four animals per cage in a 12-h light/dark cycle (lights on 0600–1800) and fed water and NIH-07 diet (11 % calories from fat; Zeigler Brothers, Inc.) ad libitum. Mice were kept separated before performing in vivo experiments. All procedures were conducted in accordance with National Institutes of Health guidelines as approved by the Animal Care and Use Committee of the National Cancer Institute.

In situ hybridization

Two sets of experiments were performed in 4-week- and 3-month-old *Anrd26*−/− and WT mice (n = 5), respectively. Mice were quickly decapitated; brains were dissected, frozen and kept at −80 °C until 8 μm serial coronal sections were cut in a cryostat and kept at −80 °C until hybridization was performed as described earlier (Young and Mezey 2004).

Finally, the sections were exposed to X-ray films and dipped in Emulsion solution (Kodak). Incubation times were determined individually using test slides and developed sequentially.

To test the specificity of the RNA probes we compared the expression pattern with previously reported normal distribution of the tested neuropeptides. The expression patterns were the same as previously reported physiological distribution in each case.

Immunohistochemistry

For immunohistochemistry (IHC), *Ankrd26*−/− mice, and age- and gender-matched WT mice were anesthetized with intraperitoneally administered Ketamine and Xylazine followed by transcardial perfusion with 1 M pH 7.2 Phosphate Buffered Saline (PBS) followed by 4 % paraformaldehyde in 1 M PBS. Brains were dissected and post-fixed overnight in the same fixative, and then incubated for 1 h in each 10 and 15 % sucrose at RT followed by an

incubation in a 20 % sucrose solution at 4 °C until they sank. 8 μm thick serial sections were cut through the brain and pituitary gland in a CM3050 S cryostat (Leica). Sections were kept at −80 °C until immunostaining, when sections were brought to room temperature, washed 3 times for 5 min in 1 M PBS and heat-unmasked in citrate buffer in a regular microwave oven. Non-specific binding sites were blocked with Power Block reagent (BioGenex Laboratories) for 10 min. Slides were incubated with primary antibody overnight at 4 °C. The following antibodies were used: rabbit polyclonal anti-ANKRD26 (1:500, SDI), goat polyclonal anti-Leptin Receptor (1:500, Sigma) chicken polyclonal anti-POMC (1:1,000, Novus Biologicals), rabbit polyclonal anti-MC4 Receptor (1:500, Abcam), rabbit polyclonal anti-adenylyl cyclase 3 (AC3) (1:500, Santa Cruz), goat polyclonal anti-Mchr1 (1:500, Santa Cruz), goat polyclonal anti-Sstr3 (1:500, Santa Cruz), rabbit polyclonal anti-Bbs2 (1:500, ProteinTech Group Inc), rabbit polyclonal anti-Bbs4 (1:500, Santa Cruz), rabbit polyclonal anti-Rootletin (1:500, Santa Cruz) and rabbit monoclonal anti-PSTAT3 (1:500, Cell Signaling). Overnight incubation with anti-AC3, anti-Mchr1, anti-Sstr3, anti-Rootletin or anti-STAT3 antibodies was followed by incubation with appropriate fluorescein-conjugated secondary antibodies (Invitrogen). For primary antibodies raised in rabbit, anti-rabbit SuperPicture (Invitrogen) was used following the manufacturer's protocol. For the rest of primary antibodies, appropriate biotin-conjugated secondary antibodies (1:1,000, Invitrogen) were used followed by 30 min incubation with streptavidin-HRP (Pierce Biotechnology). For signal amplification, FITC or Alexa 594 TSA Tyramide Kit (Invitrogen) was used following the manufacturer's recommendations. The immunostainings were visualized with a DMI6000 Leica inverted fluorescence microscope equipped with a Hamamatsu Orca camera, motorized stage and Volocity 4.01 software (Improvision, Perkin-Elmer, MA).

Micropunching and qRT PCR

Three-month-old *Ankrd26*−/− and wild-type mice were used (n = 5). Mice were decapitated and brains were quickly removed and placed on powdered dry ice. Samples were obtained by the micropunching technique (Palkovits 1983). 200 μm thick serial sections were cut and thaw-mounted onto slides in the cryostat. The slides were immediately placed on dry ice, and kept at −80 °C until needed. The micropunching was performed with a punching needle (200 μm in diameter) on dry ice, under stereomicroscopic control. Samples were obtained from the ARC, PVN and cortex, and kept in Eppendorf tubes at −80 °C until processing. Total RNA was isolated using PicoPure RNA isolation Kit from MDS Analytical Technologies in conjunction with RNase-Free DNase Set from Qiagen was used. Quantitative RT–PCR (qRT-PCR) was performed using TaqMan Universal PCR Mastermix (Applied Biosystems), Reverse Transcription Reagents using random hexamers (Applied Biosystems) and ABI 7900 HT instrument. The following TaqMan probes were used: POMC (Mm00435874_m1), AgRP (Mm00475829_g1), NPY (Mm 00445771_m1), NPY (Y1 Mm 00650798_g1), CRH (Mm012939_20_s1), MC4R (Mm 00457483_s1), while the housekeeping Pgk1 (Mm00435617_m1) was utilized as the reference gene. Quantification of the target genes mRNAs was performed using the delta cycle threshold (dC_T) method.

Determination of hypothalamic α-MSH concentration

Six-week-old *Ankrd26*−/− and WT mice were used (n = 10). Two hours after the light period onset, mice were quickly decapitated and hypothalami were carefully dissected and lysed as

described previously (Lloyd et al. 2006). α-MSH concentrations were measured by radioimmunoassay (RIA) (Phoenix Pharmaceuticals) following the manufacturer's recommendations.

STAT3 phosphorylation after leptin treatment

Six-week-old *Ankrd26*−/− and WT mice were used (n = 8). After overnight starvation and 2 h after the light period onset, the mice were intraperitoneally injected with either 3 mg/kg of recombinant mouse leptin (R&D Systems) or saline, as described earlier (Bates et al. 2003). After 35 min, mice were anesthetized and transcardially perfused (for details see Immunohistochemistry). STAT3 phosphorylation was evaluated by IHC in 8 μm thick coronal brain sections.

α-MSH administration

Three-month-old *Ankrd26*−/−, *Pomc*−/− and WT mice were used (n = 10). The α-MSH analog [Ac-Cys4, D-Phe7, Cys10] α-MSH (4–13) amide23] was obtained from Bachem.

After a 2-week-long pretreatment period, when the daily food intake and BW were monitored, mice were injected intraperitoneally once a day with 1 μg of the α-MSH analog, 1–2 h before the dark period onset for 14 days (Ref POMC−/− mice). Five *Ankrd*−/−, 5 *Pomc*−/− and 5 WT mice were administered α-MSH, while 5 mice from each genetic background received same amount of PBS. BW and food consumption were monitored daily.

Serum ACTH and corticosterone measurement

Ankrd26−/− and WT mice (n = 10) were used in each experimental group. Mice were housed separately. For the basal ACTH and corticosterone levels determination, mice were quickly decapitated 2 h after the light period onset and trunk blood was collected. For measuring ACTH and corticosterone response to stress stimulus, mice were restrained in Decapicones (Braintree scientific Inc.) for 15 min followed by quick decapitation and collection of the trunk blood. Samples were kept 30 min room temperature to let the blood coagulate. Sera were separated by 15 min centrifugation at 6 rpm and kept at −80 °C until further usage. Serum ACTH and corticosterone concentrations were determined by ELISA (ACTH, MD Bioproducts; Corticosterone, Enzo Life Sciences) following the instructions of the manufacturers.

Adrenalectomy

Adult male *Ankrd26*−/− and WT mice were used for this experiment (n = 7 in each group). For bilateral adrenalectomy, mice were anesthetized with isoflurane and 0.5 mg/kg buprenorphine administered subcutaneously and the adrenals were removed in a sterile environment.

Ankrd26−/− and WT mice (n = 14) were adrenalectomized, and half of the mice (n = 7) were given corticosterone replacement (25 mg/L) in the drinking water available ad libitum immediately after the operation. Corticosterone was purchased from Sigma (C2505),

dissolved in ethanol and diluted in 0.9 % saline to reach a 0.6 % final concentration of ethanol.

A third group of *Ankrd26*−/− and WT mice ($n = 7$) were sham operated, and underwent the same procedure as the adrenalectomized mice, when adrenal glands were exposed but not removed. The non-steroid-supplemented groups (adrenalectomized and sham-operated) were given 0.9 % saline and 0.6 % ethanol instead of regular drinking water. The water consumption was recorded every 5 days. To confirm the successful adrenalectomy and the effectiveness of the corticosterone replacement blood samples were obtained from mandibular veins from each mouse after 2 h of the onset of the light cycle and serum corticosterone levels were determined by ELISA (Enzo Life Sciences) following the manufacturer's instructions.

Statistics

Two-way ANOVA test was used to determine statistical significance. The significance level was set at $p < 0.05$.

Supplementary Material

Refer to Web version on PubMed Central for supplementary material.

Acknowledgments

The authors want to acknowledge the invaluable help of Miklos Palkovits, Harold Gainer and Michael Brownstein for their continuous support and advice as well as help with editing the manuscript. We also thank Prof. Ronald DeKloet (Leiden University) for his expert advice regarding studies on adrenal function. This research was supported by the Division of Intramural Research program of NCI and NIDCR in the Intramural Research Program, NIH, DHHS. We dedicate this work to the memory of Wylie Vale, who discovered CRF and who was an outstanding scientist; a wonderful human being and a good friend.

Abbreviations

AC3	Adenylyl cyclase 3
ACTH	Adrenocorticotrophic hormone
ADX	Adrenalectomy
α-MSH	α-Melanocyte stimulating hormone
AgRP	Agouti-related protein
Ankrd26	Ankyrin repeat domain 26
ARC	Arcuate nucleus
BBS	Bardet–Biedl syndrome
BW	Body weight
CNS	Central nervous system
CORT	Corticosterone

CRH	Corticotropin-releasing hormone
DM	Dorsomedial nucleus of the hypothalamus
GPCR	G-protein-coupled receptor
HPA	Hypothalamus–pituitary–adrenal
IHC	Immunohistochemistry
MC4R	Melanocortin 4 receptor
Mchr 1	Melanin-concentrating hormone receptor 1
NPY	Neuropeptide Y
NTS	Nucleus of the solitary tract
POMC	Proopiomelanocortin
PVN	Paraventricular nucleus of the hypothalamus
Sstr3	Somatostatin receptor 3
TRH	Thyrotropin releasing hormone
VM	Ventromedial nucleus of the hypothalamus
VP	Arginine vasopressin

References

Ansley SJ, Badano JL, Blacque OE, Hill J, Hoskins BE, Leitch CC, Kim JC, Ross AJ, Eichers ER, Teslovich TM, Mah AK, Johnsen RC, Cavender JC, Lewis RA, Leroux MR, Beales PL, Katsanis N. Basal body dysfunction is a likely cause of pleiotropic Bardet-Biedl syndrome. Nature. 2003; 425(6958):628–633. doi:10.1038/nature02030. [PubMed: 14520415]

Ao Y, Go VL, Toy N, Li T, Wang Y, Song MK, Reeve JR Jr, Liu Y, Yang H. Brainstem thyrotropin-releasing hormone regulates food intake through vagal-dependent cholinergic stimulation of ghrelin secretion. Endocrinology. 2006; 147(12):6004–6010. doi:10.1210/en.2006-0820. [PubMed: 16959836]

Arens J, Moar KM, Eiden S, Weide K, Schmidt I, Mercer JG, Simon E, Korf HW. Age-dependent hypothalamic expression of neuropeptides in wild-type and melanocortin-4 receptor-deficient mice. Physiol Genomics. 2003; 16(1):38–46. doi:10.1152/physiolgenomics.00123.2003. [PubMed: 14559977]

Bates SH, Stearns WH, Dundon TA, Schubert M, Tso AW, Wang Y, Banks AS, Lavery HJ, Haq AK, Maratos-Flier E, Neel BG, Schwartz MW, Myers MG Jr. STAT3 signalling is required for leptin regulation of energy balance but not reproduction. Nature. 2003; 421(6925):856–859. doi:10.1038/nature 01388. [PubMed: 12594516]

Beckers S, Zegers D, Van Gaal LF, Van Hul W. The role of the leptin-melanocortin signalling pathway in the control of food intake. Crit Rev Eukaryot Gene Expr. 2009; 19(4):267–287. [PubMed: 19817705]

Beckers S, Zegers D, de Freitas F, Peeters AV, Verhulst SL, Massa G, Van Gaal LF, Timmermans JP, Desager KN, Van Hul W. Identification and functional characterization of novel mutations in the melanocortin-4 receptor. Obes Facts. 2010; 3(5):304–311. doi:10.1159/000321565. [PubMed: 20975296]

Benzinou M, Walley A, Lobbens S, Charles MA, Jouret B, Fumeron F, Balkau B, Meyre D, Froguel P. Bardet-Biedl syndrome gene variants are associated with both childhood and adult common obesity

in French Caucasians. Diabetes. 2006; 55(10):2876–2882. doi:10.2337/db06-0337. [PubMed: 17003356]

Bera TK, Liu XF, Yamada M, Gavrilova O, Mezey E, Tessarollo L, Anver M, Hahn Y, Lee B, Pastan I. A model for obesity and gigantism due to disruption of the Ankrd26 gene. Proc Natl Acad Sci USA. 2008; 105(1):270–275. doi:10.1073/pnas.0710978105. [PubMed: 18162531]

Berbari NF, Johnson AD, Lewis JS, Askwith CC, Mykytyn K. Identification of ciliary localization sequences within the third intracellular loop of G protein-coupled receptors. Mol Biol Cell. 2008a; 19(4):1540–1547. doi:10.1091/mbc.E07-09-0942. [PubMed: 18256283]

Berbari NF, Lewis JS, Bishop GA, Askwith CC, Mykytyn K. Bardet-Biedl syndrome proteins are required for the localization of G protein-coupled receptors to primary cilia. Proc Natl Acad Sci USA. 2008b; 105(11):4242–4246. doi:10.1073/pnas.0711027105. [PubMed: 18334641]

Blacque OE, Leroux MR. Bardet-Biedl syndrome: an emerging pathomechanism of intracellular transport. Cell Mol Life Sci. 2006; 63(18):2145–2161. doi:10.1007/s00018-006-6180-x. [PubMed: 16909204]

Chua SC Jr, Chung WK, Wu-Peng XS, Zhang Y, Liu SM, Tartaglia L, Leibel RL. Phenotypes of mouse diabetes and rat fatty due to mutations in the OB (leptin) receptor. Science. 1996; 271(5251):994–996. [PubMed: 8584938]

Collin GB, Marshall JD, Ikeda A, So WV, Russell-Eggitt I, Maffei P, Beck S, Boerkoel CF, Sicolo N, Martin M, Nishina PM, Naggert JK. Mutations in ALMS1 cause obesity, type 2 diabetes and neurosensory degeneration in Alstrom syndrome. Nat Genet. 2002; 31(1):74–78. doi:10.1038/ng867. [PubMed: 11941369]

de Backer MW, la Fleur SE, Brans MA, van Rozen AJ, Luijendijk MC, Merkestein M, Garner KM, van der Zwaal EM, Adan RA. Melanocortin receptor-mediated effects on obesity are distributed over specific hypothalamic regions. Int J Obes (Lond). 2011; 35(5):629–641. doi:10.1038/ijo.2010.169. [PubMed: 20733584]

Dimitrov EL, DeJoseph MR, Brownfield MS, Urban JH. Involvement of neuropeptide Y Y1 receptors in the regulation of neuroendocrine corticotropin-releasing hormone neuronal activity. Endocrinology. 2007; 148(8):3666–3673. doi:10.1210/en.2006-1730. [PubMed: 17463058]

Dong C, Li WD, Geller F, Lei L, Li D, Gorlova OY, Hebebrand J, Amos CI, Nicholls RD, Price RA. Possible genomic imprinting of three human obesity-related genetic loci. Am J Hum Genet. 2005; 76(3):427–437. doi:10.1086/428438. [PubMed: 15647995]

Friedman JM. Obesity in the new millennium. Nature. 2000; 404(6778):632–634. doi:10.1038/35007504. [PubMed: 10766249]

Friedman JM, Halaas JL. Leptin and the regulation of body weight in mammals. Nature. 1998; 395(6704):763–770. doi:10.1038/27376. [PubMed: 9796811]

Goldstone AP, Beales PL. Genetic obesity syndromes. Front Horm Res. 2008; 36:37–60. doi:10.1159/0000115336. [PubMed: 18230893]

Grace C, Beales P, Summerbell C, Jebb SA, Wright A, Parker D, Kopelman P. Energy metabolism in Bardet-Biedl syndrome. Int J Obes Relat Metab Disord. 2003; 27(11):1319–1324. doi:10.1038/sj.ijo.0802420. [PubMed: 14574341]

Grill HJ, Hayes MR. The nucleus tractus solitarius: a portal for visceral afferent signal processing, energy status assessment and integration of their combined effects on food intake. Int J Obes (Lond). 2009; 33(Suppl 1):S11–S15. doi:10.1038/ijo.2009.10. [PubMed: 19363500]

Guo DF, Rahmouni K. Molecular basis of the obesity associated with Bardet-Biedl syndrome. Trends Endocrinol Metab: TEM. 2011; 22(7):286–293. doi:10.1016/j.tem.2011.02.009. [PubMed: 21514177]

Harris M, Aschkenasi C, Elias CF, Chandrankunnel A, Nillni EA, Bjoorbaek C, Elmquist JK, Flier JS, Hollenberg AN. Transcriptional regulation of the thyrotropin-releasing hormone gene by leptin and melanocortin signaling. J Clin Invest. 2001; 107(1):111–120. doi:10.1172/jci10741. [PubMed: 11134186]

Huszar D, Lynch CA, Fairchild-Huntress V, Dunmore JH, Fang Q, Berkemeier LR, Gu W, Kesterson RA, Boston BA, Cone RD, Smith FJ, Campfield LA, Burn P, Lee F. Targeted disruption of the melanocortin-4 receptor results in obesity in mice. Cell. 1997; 88(1):131–141. [PubMed: 9019399]

Itoi K, Jiang YQ, Iwasaki Y, Watson SJ. Regulatory mechanisms of corticotropin-releasing hormone and vasopressin gene expression in the hypothalamus. J Neuroendocrinol. 2004; 16(4):348–355. doi:10.1111/j.0953-8194.2004.01172.x. [PubMed: 15089973]

Kim JC, Badano JL, Sibold S, Esmail MA, Hill J, Hoskins BE, Leitch CC, Venner K, Ansley SJ, Ross AJ, Leroux MR, Katsanis N, Beales PL. The Bardet-Biedl protein BBS4 targets cargo to the pericentriolar region and is required for microtubule anchoring and cell cycle progression. Nat Genet. 2004; 36(5):462–470. doi:10.1038/ng1352. [PubMed: 15107855]

Kiss JZ, Mezey E, Skirboll L. Corticotropin-releasing factor-immunoreactive neurons of the paraventricular nucleus become vasopressin positive after adrenalectomy. Proc Natl Acad Sci USA. 1984; 81(6):1854–1858. [PubMed: 6608732]

Leibowitz SF, Hammer NJ, Chang K. Hypothalamic paraventricular nucleus lesions produce overeating and obesity in the rat. Physiol Behav. 1981; 27(6):1031–1040. [PubMed: 7335803]

Lloyd DJ, Bohan S, Gekakis N. Obesity, hyperphagia and increased metabolic efficiency in Pc1 mutant mice. Hum Mol Genet. 2006; 15(11):1884–1893. doi:10.1093/hmg/ddl111. [PubMed: 16644867]

Lu XY, Barsh GS, Akil H, Watson SJ. Interaction between alpha-melanocyte-stimulating hormone and corticotropin-releasing hormone in the regulation of feeding and hypothalamopituitary-adrenal responses. J Neurosci. 2003; 23(21):7863–7872. [PubMed: 12944516]

Mercer RE, Chee MJ, Colmers WF. The role of NPY in hypothalamic mediated food intake. Front Neuroendocrinol. 2011 doi:10.1016/j.yfrne.2011.06.001.

Nakayama S, Nishiyama M, Iwasaki Y, Shinahara M, Okada Y, Tsuda M, Okazaki M, Tsugita M, Taguchi T, Makino S, Stenzel-Poore MP, Hashimoto K, Terada Y. Corticotropin-releasing hormone (CRH) transgenic mice display hyperphagia with increased Agouti-related protein mRNA in the hypothalamic arcuate nucleus. Endocr J. 2011; 58(4):279–286. [PubMed: 21389639]

Nordman S, Abulaiti A, Hilding A, Langberg EC, Humphreys K, Ostenson CG, Efendic S, Gu HF. Genetic variation of the adenylyl cyclase 3 (AC3) locus and its influence on type 2 diabetes and obesity susceptibility in Swedish men. Int J Obes (Lond). 2008; 32(3):407–412. doi:10.1038/sj.ijo.0803742. [PubMed: 17895882]

Palkovits M. Isolated removal of hypothalamic or other brain nuclei of the rat. Brain Res. 1973; 59:449–450. [PubMed: 4747772]

Palkovits M. Punch sampling biopsy technique. Methods Enzymol. 1983; 103:368–376. [PubMed: 6366460]

Palkovits M. Stress-induced activation of neurons in the ventromedial arcuate nucleus: a blood-brain-CSF interface of the hypothalamus. Ann N Y Acad Sci. 2008; 1148:57–63. doi:10.1196/annals.1410.062. [PubMed: 19120091]

Pandit R, de Jong JW, Vanderschuren LJ, Adan RA. Neurobiology of overeating and obesity: the role of melanocortins and beyond. Eur J Pharmacol. 2011; 660(1):28–42. doi:10.1016/j.ejphar.2011.01.034. [PubMed: 21295024]

Raciti GA, Bera TK, Gavrilova O, Pastan I. Partial inactivation of Ankrd26 causes diabetes with enhanced insulin responsiveness of adipose tissue in mice. Diabetologia. 2011 doi:10.1007/s00125-011-2263-9.

Rahmouni K, Fath MA, Seo S, Thedens DR, Berry CJ, Weiss R, Nishimura DY, Sheffield VC. Leptin resistance contributes to obesity and hypertension in mouse models of Bardet-Biedl syndrome. J Clin Invest. 2008; 118(4):1458–1467. doi:10.1172/jci32357. [PubMed: 18317593]

Ramachandrappa S, Farooqi IS. Genetic approaches to understanding human obesity. J Clin Invest. 2011; 121(6):2080–2086. doi:10.1172/jci46044. [PubMed: 21633175]

Sabatier N, Caquineau C, Dayanithi G, Bull P, Douglas AJ, Guan XM, Jiang M, Van der Ploeg L, Leng G. Alpha-melanocyte-stimulating hormone stimulates oxytocin release from the dendrites of hypothalamic neurons while inhibiting oxytocin release from their terminals in the neurohypophysis. J Neurosci. 2003; 23(32):10351–10358. [PubMed: 14614094]

Saito Y, Cheng M, Leslie FM, Civelli O. Expression of the melanin-concentrating hormone (MCH) receptor mRNA in the rat brain. J Comp Neurol. 2001; 435(1):26–40. [PubMed: 11370009]

Savontaus E, Conwell IM, Wardlaw SL. Effects of adrenalectomy on AGRP, POMC, NPY and CART gene expression in the basal hypothalamus of fed and fasted rats. Brain Res. 2002; 958(1):130–138. [PubMed: 12468037]

Sawchenko PE, Swanson LW, Vale WW. Co-expression of corticotropin-releasing factor and vasopressin immunoreactivity in parvocellular neurosecretory neurons of the adrenalectomized rat. Proc Natl Acad Sci USA. 1984; 81(6):1883–1887. [PubMed: 6369332]

Sebag JA, Hinkle PM. Regulation of endogenous melanocortin-4 receptor expression and signaling by glucocorticoids. Endocrinology. 2006; 147(12):5948–5955. doi:10.1210/en.2006-0984. [PubMed: 16973723]

Sen Gupta P, Prodromou NV, Chapple JP. Can faulty antennae increase adiposity? The link between cilia proteins and obesity. J Endocrinol. 2009; 203(3):327–336. doi:10.1677/joe-09-0116. [PubMed: 19460851]

Seo S, Guo DF, Bugge K, Morgan DA, Rahmouni K, Sheffield VC. Requirement of Bardet-Biedl syndrome proteins for leptin receptor signaling. Hum Mol Genet. 2009; 18(7):1323–1331. doi:10.1093/hmg/ddp031. [PubMed: 19150989]

Seo S, Zhang Q, Bugge K, Breslow DK, Searby CC, Nachury MV, Sheffield VC. A novel protein LZTFL1 regulates ciliary trafficking of the BBSome and smoothened. PLoS Genet. 2011; 7(11):e1002358. doi:10.1371/journal.pgen.1002358. [PubMed: 22072986]

Singla V, Reiter JF. The primary cilium as the cell's antenna: signaling at a sensory organelle. Science. 2006; 313(5787):629–633. doi:10.1126/science.1124534. [PubMed: 16888132]

Stofkova A, Skurlova M, Kiss A, Zelezna B, Zorad S, Jurcovicova J. Activation of hypothalamic NPY, AgRP, MC4R, AND IL-6 mRNA levels in young Lewis rats with early-life diet-induced obesity. Endocr Regul. 2009; 43(3):99–106. [PubMed: 19817504]

Tung YC, Piper SJ, Yeung D, O'Rahilly S, Coll AP. A comparative study of the central effects of specific proopiomelancortin (POMC)-derived melanocortin peptides on food intake and body weight in pomc null mice. Endocrinology. 2006; 147(12):5940–5947. doi:10.1210/en.2006-0866. [PubMed: 16959830]

Valassi E, Scacchi M, Cavagnini F. Neuroendocrine control of food intake. Nutr Metab Cardiovasc Dis. 2008; 18(2):158–168. doi:10.1016/j.numecd.2007.06.004. [PubMed: 18061414]

Wang Z, Li V, Chan GC, Phan T, Nudelman AS, Xia Z, Storm DR. Adult type 3 adenylyl cyclase-deficient mice are obese. PLoS ONE. 2009; 4(9):e6979. doi:10.1371/journal.pone.0006979. [PubMed: 19750222]

Wardlaw SL. Hypothalamic proopiomelanocortin processing and the regulation of energy balance. Eur J Pharmacol. 2011; 660(1):213–219. doi:10.1016/j.ejphar.2010.10.107. [PubMed: 21208604]

Wardle J, Carnell S, Haworth CM, Plomin R. Evidence for a strong genetic influence on childhood adiposity despite the force of the obesogenic environment. Am J Clin Nutr. 2008; 87(2):398–404. [PubMed: 18258631]

Yang J, Li T. The ciliary rootlet interacts with kinesin light chains and may provide a scaffold for kinesin-1 vesicular cargos. Exp Cell Res. 2005; 309(2):379–389. doi:10.1016/j.yexcr.2005.05.026. [PubMed: 16018997]

Yang J, Liu X, Yue G, Adamian M, Bulgakov O, Li T. Rootletin, a novel coiled-coil protein, is a structural component of the ciliary rootlet. J Cell Biol. 2002; 159(3):431–440. doi:10.1083/jcb.200207153. [PubMed: 12427867]

Yang L, Scott KA, Hyun J, Tamashiro KL, Tray N, Moran TH, Bi S. Role of dorsomedial hypothalamic neuropeptide Y in modulating food intake and energy balance. J Neurosci. 2009; 29(1):179–190. doi:10.1523/jneurosci.4379-08.2009. [PubMed: 19129396]

Yaswen L, Diehl N, Brennan MB, Hochgeschwender U. Obesity in the mouse model of pro-opiomelanocortin deficiency responds to peripheral melanocortin. Nat Med. 1999; 5(9):1066–1070. doi:10.1038/12506. [PubMed: 10470087]

Young WS 3rd, Mezey E. Hybridization histochemistry of neural transcripts. Curr Protoc Neurosci. 2004; Chapter 1(Unit 1):3. doi:10.1002/0471142301.ns0103s25. [PubMed: 18428597]

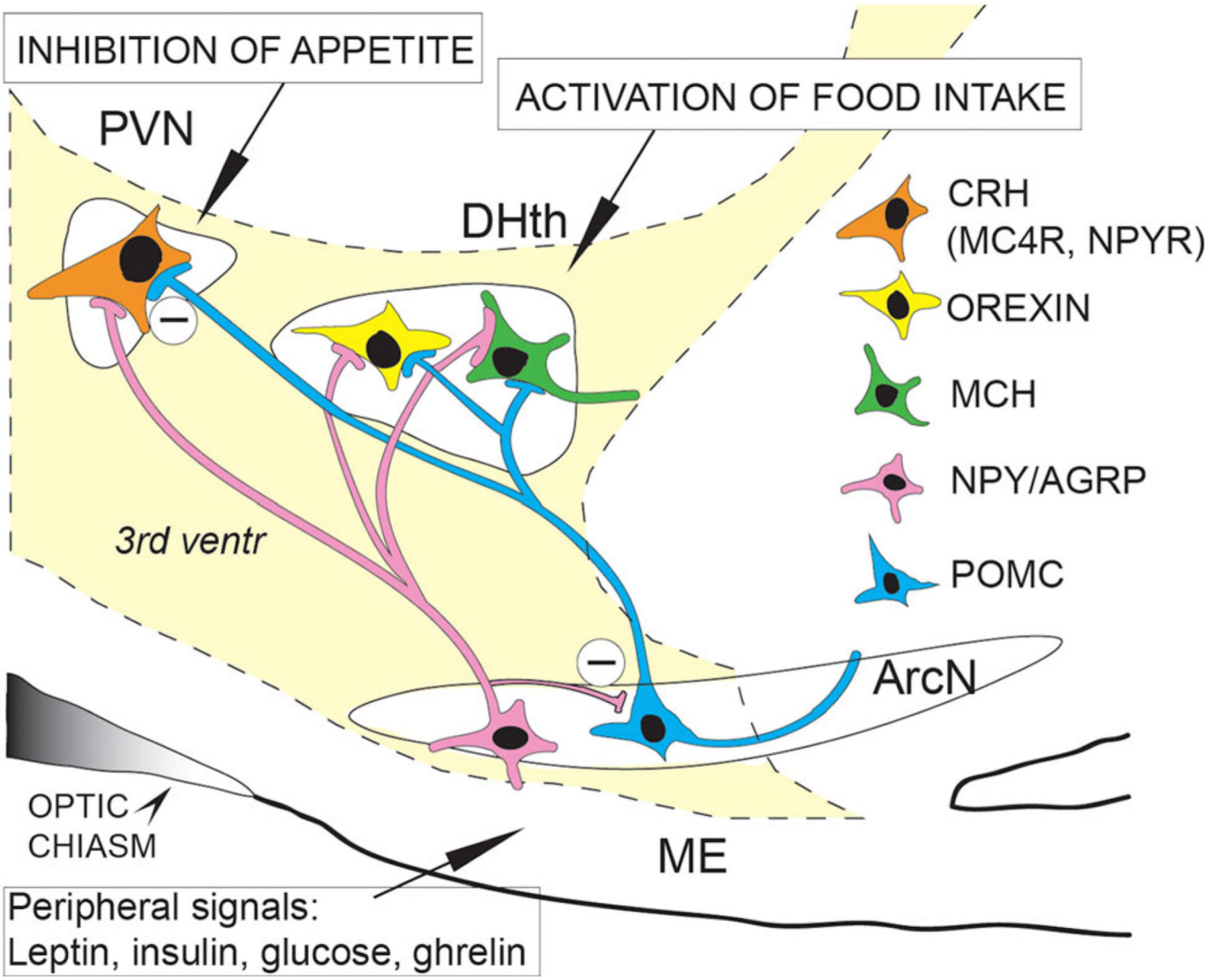

Fig. 1.

Schematic demonstration of the hypothalamic regulation of appetite. Peripheral satiety hormones reach POMC and NPY/AGRP neuron groups in the arcuate nucleus (ArcN) of the hypothalamus. Activation of POMC neurons by anorexigenic hormones (e.g., leptin) stimulates the hypothalamic MC4 receptor-expressing cells (e.g., CRH neurons) inhibiting appetite, while orexigenic NPY/AGRP neurons in the arcuate nucleus and the dorsomedial hypothalamus (DHth) are inhibited. In contrast, when orexigenic satiety signals (e.g., ghrelin) activate NPY/AGRP neurons, the dorsomedial hypothalamus is stimulated and the activity of PVN neurons is attenuated. As a result food intake increases. *PVN* paraventricular nucleus, *ME* median eminence, *3rd ventr* third ventricle, *CRH* corticotrophin-releasing hormone, *MC4R* melanocortin 4 receptor, *NPYR* NPY receptor, *MCH* melanine-concentrating hormone. (Modified from M. Palkovits)

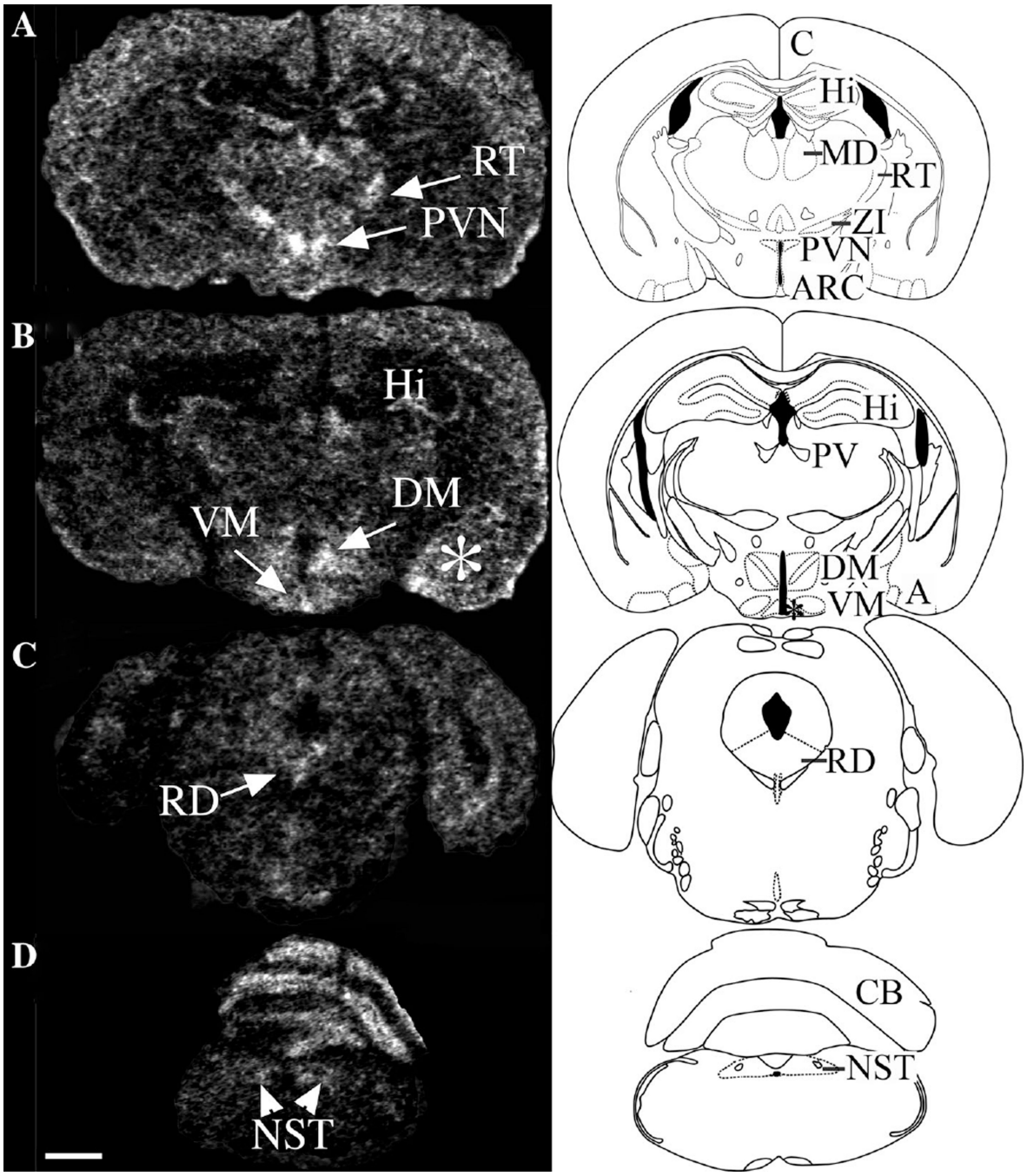

Fig. 2.

Expression of *Ankrd26* mRNA in the mouse brain. Inverted X-ray image of in situ hybridization demonstrates the distribution of *Ankrd26* mRNA in the brain. *Left panel* representative in situ hybridization images from different brain areas. *Right panel* schematic drawings of the corresponding brain areas. Areas with marked *Ankrd26* mRNA expression are indicated in the schematic drawings by abbreviations. **a** *Ankrd26* expression in the cortex (**c**), hippocampal CA2 and CA3 regions (Hi), mediodorsal thalamic nucleus (MD), reticular thalamic nucleus (RT), zona incerta (ZI), and in the hypothalamic PVN and ARC. **b**

Prominent signal detected in the hippocampal CA2 and CA3 regions (Hi), paraventricular thalamic nucleus (PV), medial amygdaloid nucleus and posteromedial cortical amygdaloid nucleus (**a**), and in the hypothalamic DM, VM and ARC (indicated by *asterisk*) nuclei. **c** Midbrain. Raphe dorsalis nucleus (RD) shows high signal. **d** Medulla oblongata. The nucleus of the solitary tract (NTS) and the cerebellum (CB) has visible radiolabeling. *Scale bar* 1 mm

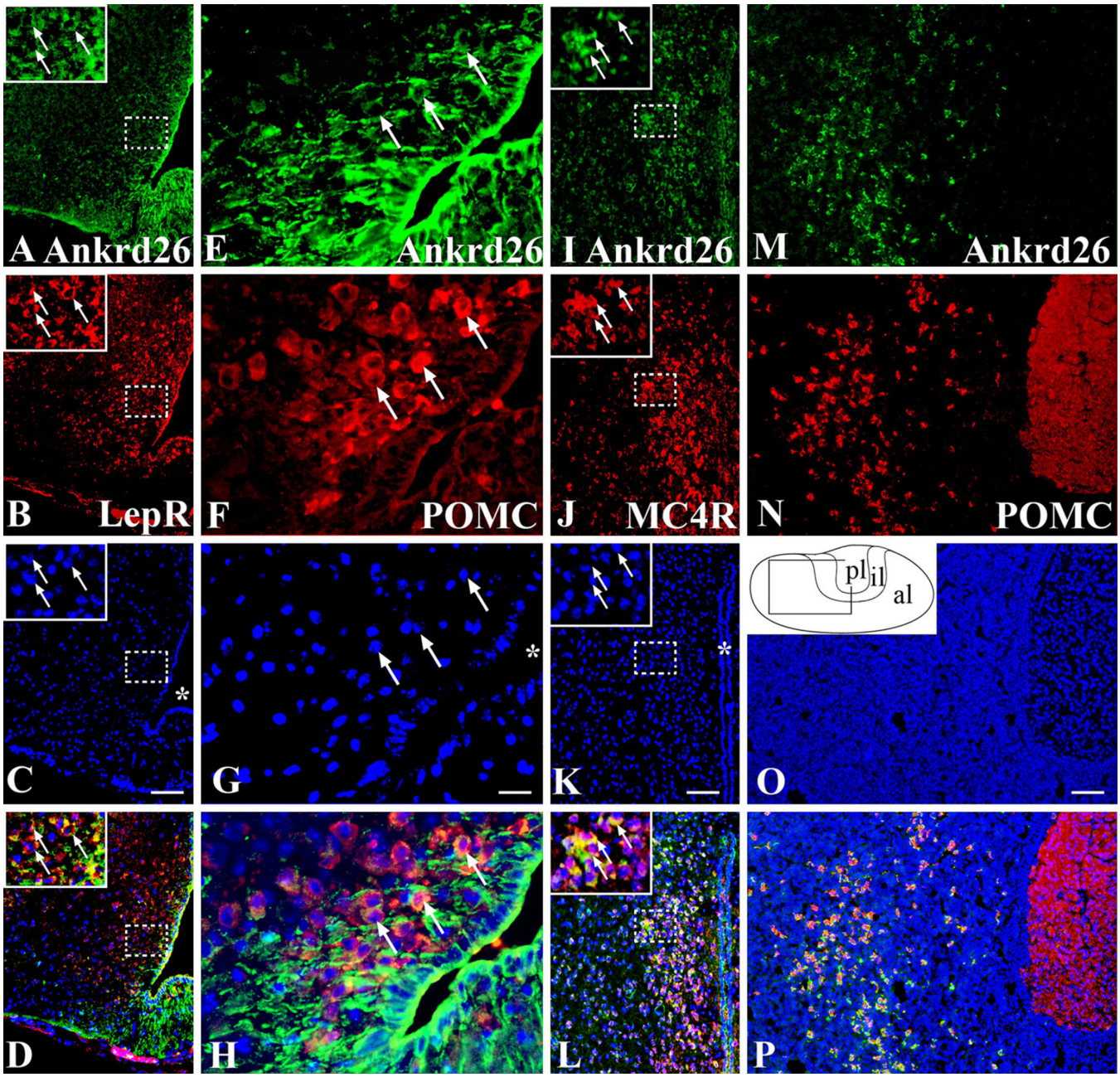

Fig. 3.

Expression of Ankrd26 in the melanocortin pathway and in the pituitary gland. Dual labeling IHC demonstrating Ankrd26 expression in the key cell populations of the melanocortin pathway. Ankrd26 immunostaining (*green*) is shown in the *upper row* (**a, e, i, m**). **a–d** In the ARC, LepR-positive cells (**b**, *red*) are co-labeled with Ankrd26 (**a**, *green*) as shown in the merged image (**d**). The magnified area in the *insets* is indicated by *dashed boxes*. *Arrows* show double-labeled cells. *Scale bar* 100 μm. **e–h** Immunostaining for POMC (**f**, *red*) and Ankrd26 (**e**, *green*) in the ARC shows many double-labeled cells (**h**, *merged image*) (*marked by arrows*). 409 magnification, *scale bar* 15 μm. **i–l** Immunostaining for MC4R (**j**, *red*) and Ankrd26 (**i**, *green*) in the PVN reveals numerous

double-stained cells (**l**, *merged image*). The magnified area in the *insets* is indicated by *dashed boxes*. *Arrows* show double-labeled cells. *Scale bar* 100 μm. **m–p** In the anterior lobe of the pituitary gland all POMC-positive cells (**n**, *red*) are stained for Ankrd26 (**p**, *merged image*). *Scale bar* 100 μm. *Inset* in **o** is the schematic drawing of the pituitary gland. *Al* anterior lobe, *il* intermediate lobe, *pl* posterior lobe. In **c, g, k** and **o** nuclei are visualized with DAPI (*blue*). *Asterisk* in **c, g**, and **k** indicates the third ventricle

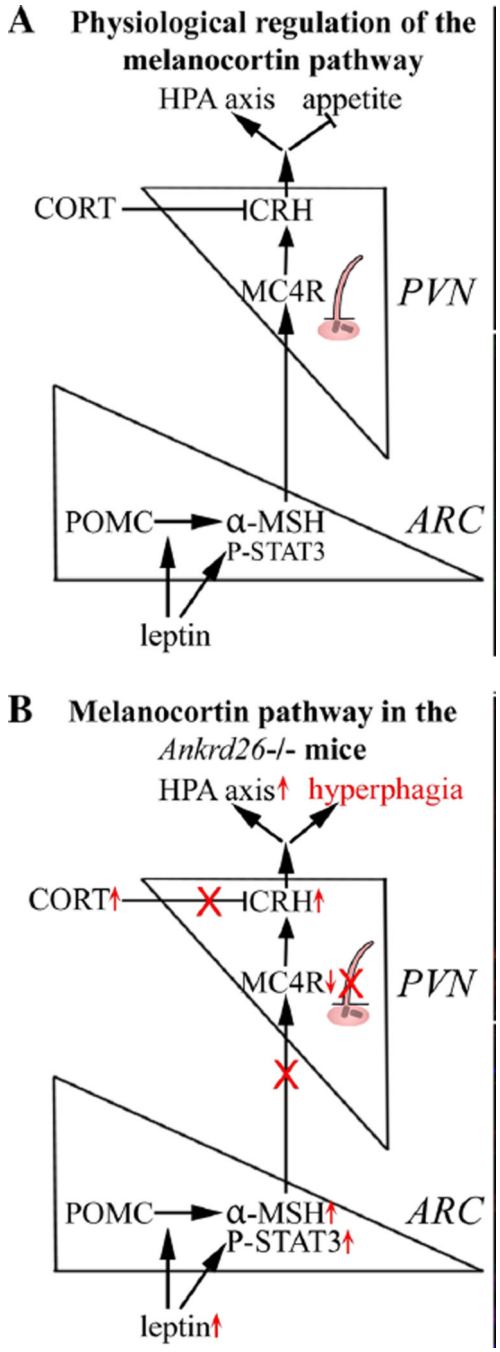

Fig. 4.

Schematic drawing summarizing the physiological regulation of the melanocortin pathway and pathological findings in the in *Ankrd26*−/− mice. **a** Under physiological conditions leptin activates STAT3 phosphorylation and POMC is cleaved to α-MSH in ARC POMC neurons. α-MSH activates MC4R-expressing CRH-producing neurons in the PVN. As a result, appetite is inhibited and the stress axis is activated. The stress response is terminated by the negative feedback of CORT. **b** In *Ankrd26*−/− mice higher leptin levels are accompanied by STAT3 phosphorylation and increase in hypothalamic α-MSH. In spite of

reduced MC4R mRNA in the PVN and elevated serum CORT levels, CRH expression is increased. This is associated with hyperphagia and overactivation of the stress pathway in *Ankrd26*−/− mice. Note, that neurons with MC4 receptors that make CRH in the PVN are ciliated. In *Ankrd26* knockout mice, these PVN cells lack AC3 positive primary cilia (see Fig. 10)

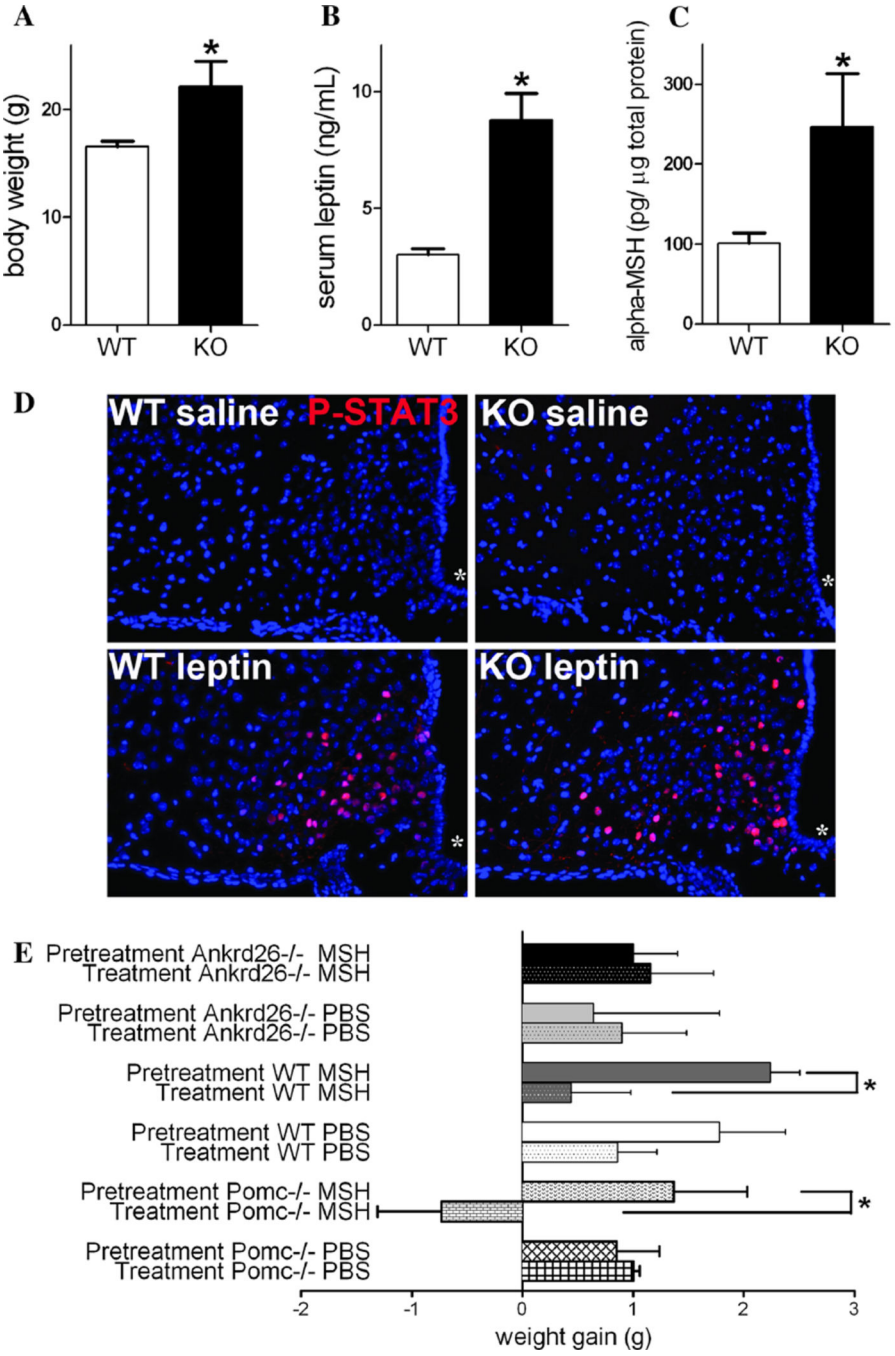

Fig. 5.

Characterization of the melanocortin pathway in *Ankrd26*−/− and WT mice. **a– c** *Graphs* show that at the age of 6 weeks, the significantly higher body weight of the *Ankrd26*−/− (KO) mice (**a**) is accompanied by significantly elevated serum leptin levels (**b**) and hypothalamic α-MSH concentration (**c**) as compared to the WT mice. Data are representative of 2 individual observations ($n = 5$ in each groups, from 2 different litters). Values are expressed as mean ± SEM. *$p < 0.05$. **d** IHC demonstrates nuclear labeling of phospho-STAT3 (*red*) in the ARC in leptintreated WT and *Ankrd26*−/− (KO) mice. *Scale*

bar 100 μm. *Asterisk* indicates the third ventricle. **e** Effect of α-MSH treatment on the body weight of *Ankrd26*−/−, *Pomc*−/− and WT mice. Comparison of weight gain in experimental groups in the pretreatment period and during the α-MSH treatment is shown. The weight gain during the pretreatment and the α-MSH treatment period was significantly less in the WT than in the *Ankrd26*−/− mice. *Pomc*−/− mice lost body weight during α-MSH administration. Data are representative of 2 individual observations ($n = 5$ in each groups, from 2 different litters). For each experiment, values are expressed as mean ± SEM. *$p < 0.05$

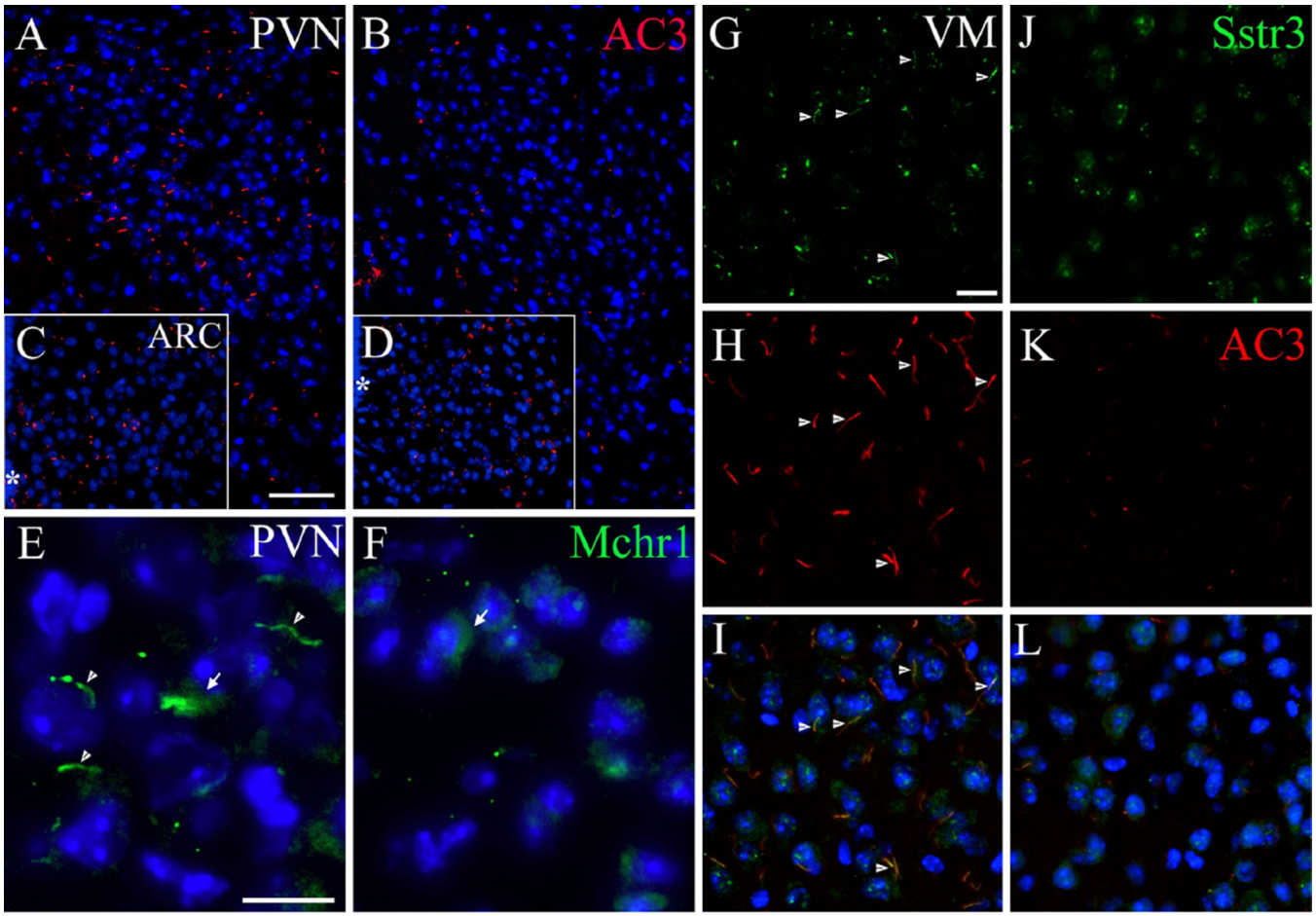

Fig. 6.

Expression of primary ciliary markers in the feeding centers in *Ankrd26*−/− and WT mice. **a, b** Show immunostaining of AC3 in the PVN of the WT (**a**) and *Ankrd26*−/− (**b**) mice. Note the almost absent immunolabeling in the PVN of the *Ankrd26*−/− mice. **c, d** The number of AC3-positive primary cilia is comparable in the ARC in WT (**c**) and *Ankrd26*−/− (**d**) mice. *Scale bar* 60 μm. *Asterisk* indicates the third ventricle. **e–f** IHC of Mchr1 (*green*) in the PVN in WT and *Ankrd26*−/− mice. **e** Neurons of the PVN express Mchr1 in the primary cilia (*arrowhead*) and in the cytoplasm (*arrow*). **f** *Ankrd26*−/− mice lack Mchr1-positive primary cilia in this region, but the immunostaining is present in the cytoplasm (*arrow*). *Scale bar* 10 μm. **g–l** Expression of Sstr3 (*green*) and AC3 (*red*) in the VM nucleus in WT (**g–i**) and in *Ankrd26*−/− (**j–l**) mice. **g, j** In WT mice (**g**) Sstr3 is localized to the primary cilia (*arrows*) and to the cytoplasm, while in the *Ankrd26*−/− mice **(j)** the ciliary staining is almost absent. **h, k** Numerous AC3-positive primary cilia are present in the WT mice (**h**), while reduced number and shorter AC3-positive primary cilia can be seen in the *Ankrd26*−/− mice (**k**). **i, l** *Merged images* indicate numerous Sstr3 and AC3 co-labeled primary cilia in the WT mice (**i**). In *Ankrd26*−/− mice (**l**) the number of Sstr3 and AC3-positive primary cilia is markedly reduced. *Scale bar* 15 μm. Nuclei are visualized with DAPI (*blue*). Images are representative of four independent observations (n = 3 in each group, four different litters)

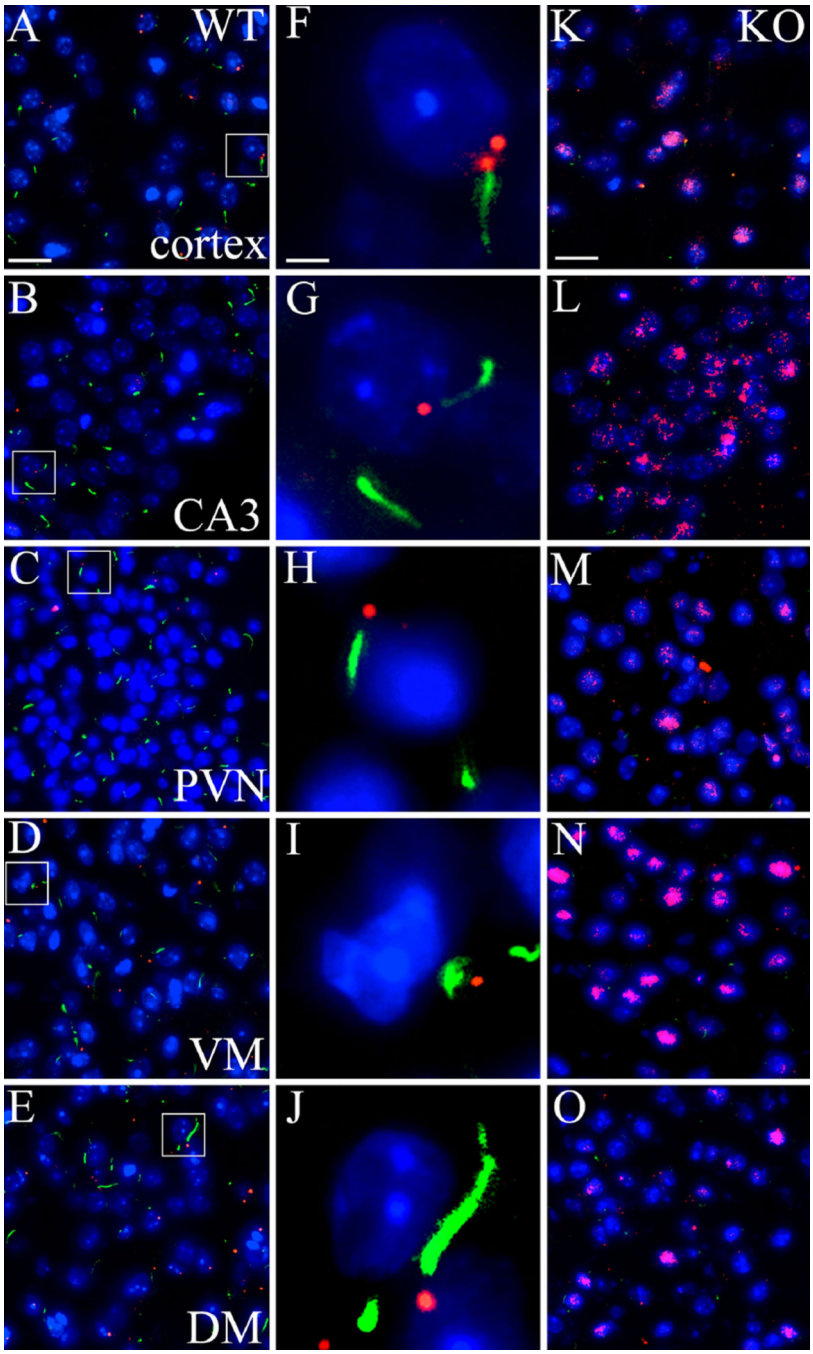

Fig. 7.

Expression and distribution of BBSome protein Bbs4 in the brain of *Ankrd26*−/− and WT mice. IHC demonstrates the expression and staining pattern of Bbs4 (*red*) and AC3 (*green*) in WT (**a–j**) and *Ankrd26*−/− (**k–o**) mice. The *middle panel* (**f–j**) displays representative cells from WT mice (*white boxes* in **a–e**). **a, f, k** represent the cortex, **b, g, l** the CA3 region of the hippocampus, **c, h, m** the PVN, **d, i, n** the VM and **e, j, o** the DM. Note the punctate staining of Bbs4 in the WT mice, the labeling is often localized to the base of AC3-positive primary cilia, as demonstrated in the middle panels (**f–j**). Bbs4 immunostaining in

Ankrd26−/− mice shows a strong nuclear/perinuclear pattern in the indicated areas, accompanied by a significantly reduced number of AC3-positive primary cilia. Nuclei are visualized with DAPI (*blue*). *Scale bar* 15 μm in **a and k**, 2 μm in **f**. Images are representative of four independent observations (n = 3 in each group, four different litters)

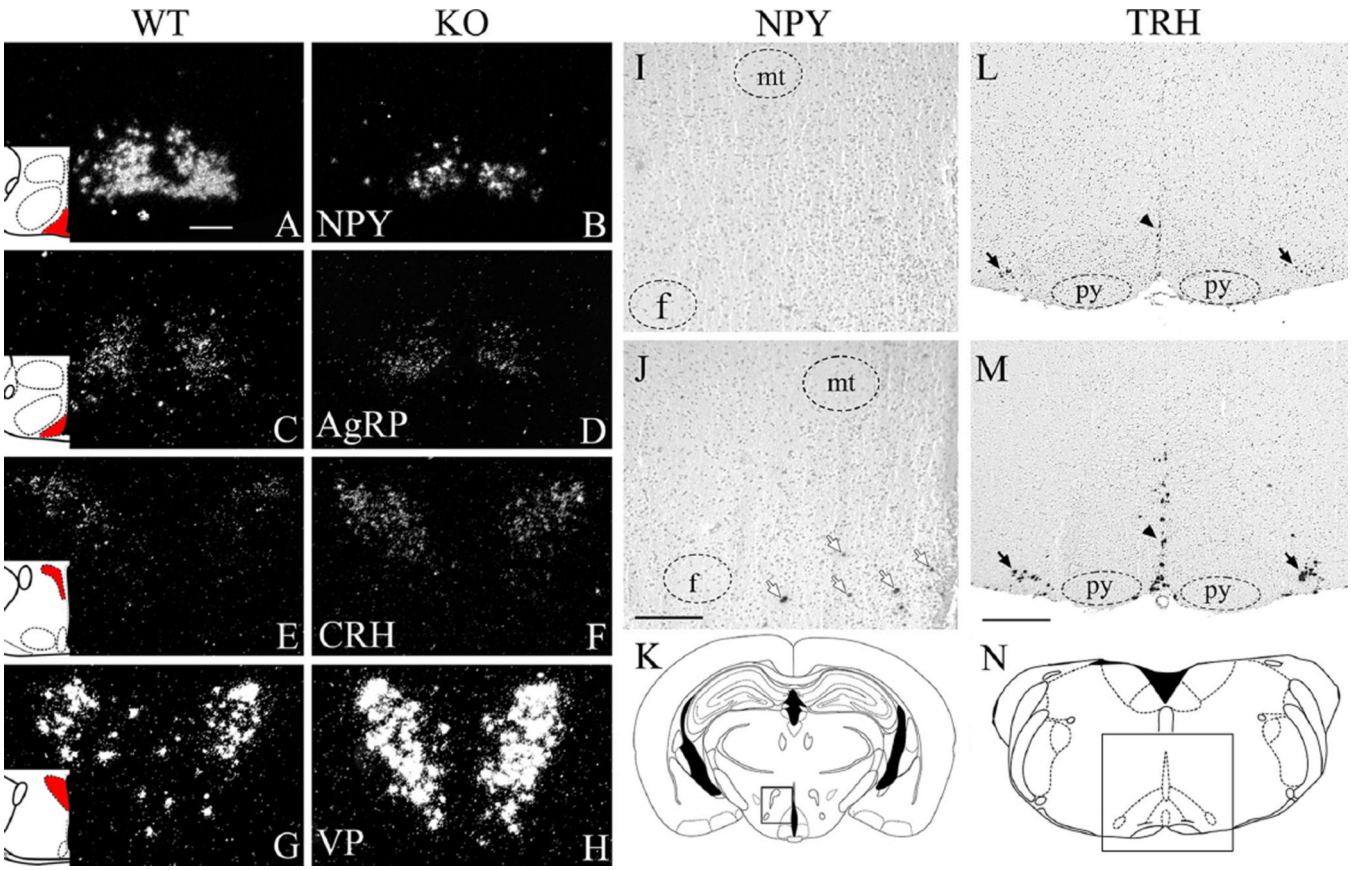

Fig. 8.

Expression of appetite- and stress-related neuropeptides in *Ankrd26*−/− and WT mice. **a–h** Representative autoradiographs demonstrate mRNA expression of neuropeptides in WT and *Ankrd26*−/− (KO) mice at 4 weeks. NPY (**a–b**) and AgRP (**c–d**) are expressed in the ARC. CRH (**e–f**) and AVP (**g–h**) are expressed in the PVN. Note that in the *Ankrd26*−/− mice, the number of NPY (**b**) and AgRP (**d**) cells and the signal intensity is reduced. CRH− (**f**) and VP− (**h**) positive cells in the PVN in the *Ankrd26*−/− mice. *Red* areas in the schematic *insets* indicate the corresponding brain areas. *Dark* field microscopy images, *scale bar* 200 μm. **i–n** Representative autoradiographs demonstrate neuropeptides mRNA expression in WT (*upper panel*, **i and l**) and *Ankrd26*−/− (**j, m**) mice at 3 months. **i–k** Images show absence of NPY in the hypothalamic DM in the WT mice (**i**), while many NPY-positive cells are present here in the *Ankrd26*−/− mice (**j**). *Arrows* indicate NPY-positive cells. *mt* mammillothalamic tract, *f* fornix. *Scale bar* 200 μm. **k** The *box* in the schematic drawing demonstrates the corresponding brain area. **l–n** TRH-expressing neurons are present in the brainstem (raphe obscurus, raphe pallidus and parapyramidal nuclei) in the WT (**l**) and *Ankrd*26−/− (**m**) mice. Note that the number of TRH-positive cells and the intensity of the signal are increased in the *Ankrd26*−/− (**m**) mice. *Arrows* indicate the parapyramidal nucleus; *arrowheads* indicate the midline raphe nuclei. (**n**) The *box* in the schematic drawing demonstrates the corresponding brain area. Py, pyramidal tract. *Scale bar* 500 μm. Bright field microscopy images

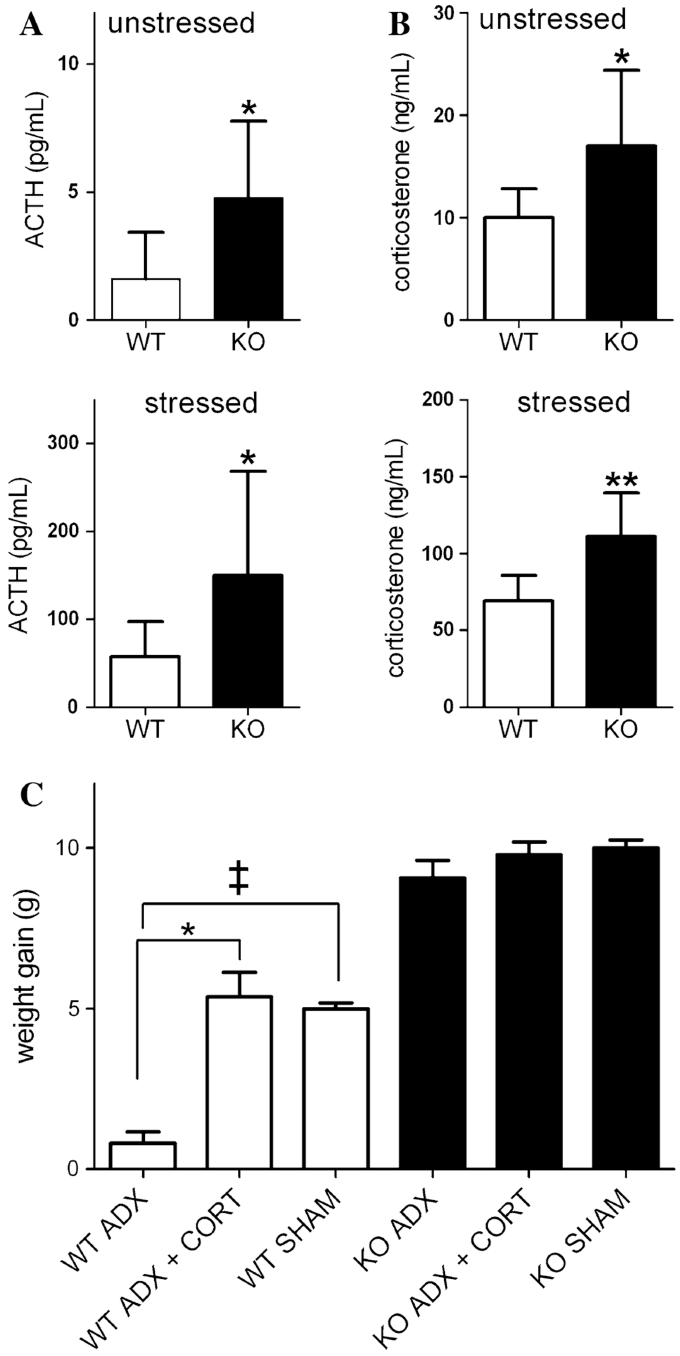

Fig. 9.

Characterization of the HPA axis in *Ankrd26*−/− and WT mice. **a, b** Serum ACTH and CORT levels of *Ankrd26*−/− and WT mice. **a** *Upper panel* basal levels of serum ACTH in *Ankrd26*−/− (KO) and WT mice. *Lower panel* serum ACTH levels following 15 min of restraint stress. **b** *Upper panel* basal levels of serum CORT in *Ankrd26*−/− (KO) and WT mice. *Lower panel* serum CORT levels after 15 min of restraint stress. Bars represent mean values (n = 10 for each group) ± SEM. **p* < 0.05, ***p* < 0.01. **c** Effect of adrenalectomy on the body weight of *Ankrd26*−/− and WT mice. Weight gain of experimental mice from day

14 until the end of the experiment is demonstrated. Note, that the body weight gain of the *Ankrd26*−/− mice is comparable in each group, while CORT-supplemented (ADX + CORT) and sham-operated WT mice gained significantly more weight compared to the non-replaced WT mice (ADX). *$p < 0.05$ WT ADX + CORT vs. WT ADX, ‡$p < 0.05$ WT SHAM vs. WT ADX. Values are expressed as mean ± SEM ($n = 7$ in each group)

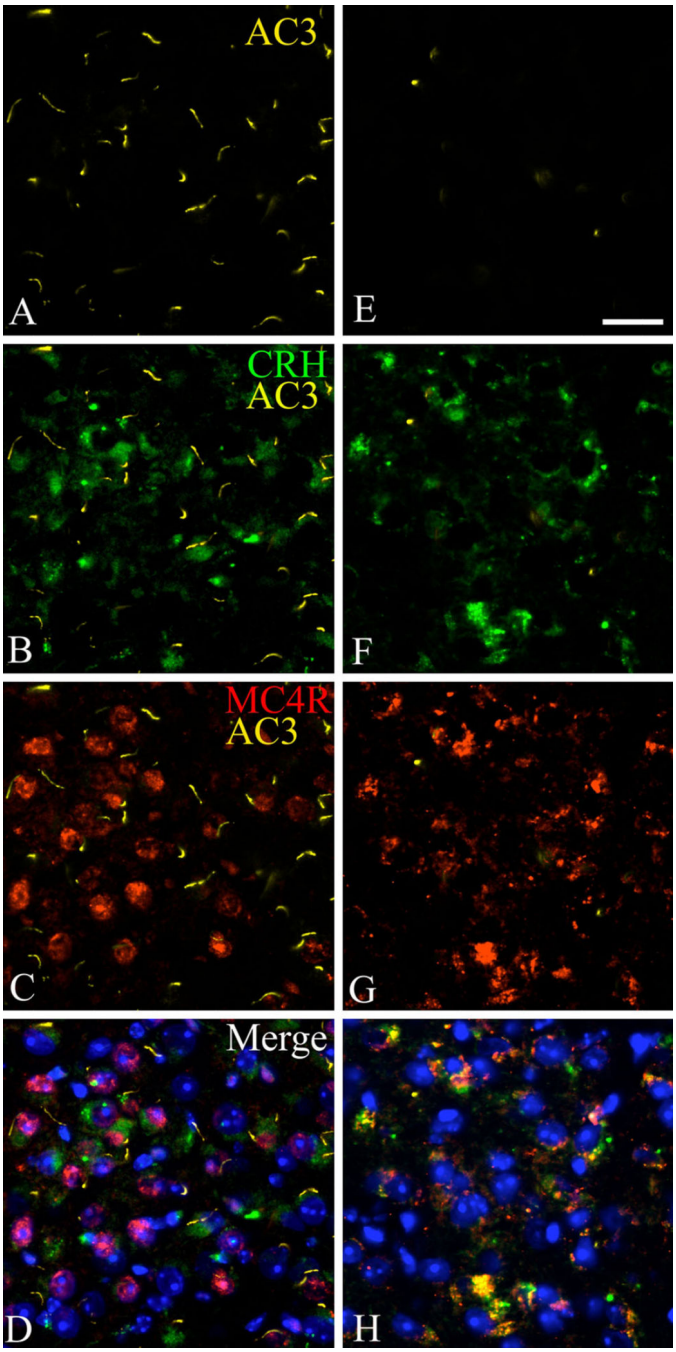

Fig. 10.

The expression of AC3 primary ciliary marker in the CRH neurons in the PVN in *Ankrd26*−/− and WT mice. Triple IHC demonstrates that in WT mice (**a–d**) CRH-producing (**b**, *green*) MC4R-expressing (**c**, *red*) cells in the PVN express AC3 (**a**, *yellow*). This cell population lacks AC3-positive primary cilia in *Ankrd26*−/− mice (**e–h**). Nuclei are visualized with DAPI (*blue*). 409 magnification; *scale bar* 15 μm; *n* = 3 in each group